THE CHEMICAL RECORD

Saccharomyces cerevisiae Oxidosqualene-Lanosterol Cyclase: A Chemistry–Biology Interdisciplinary Study of the Protein's Structure–Function–Reaction Mechanism Relationships

TUNG-KUNG WU, CHENG-HSIANG CHANG, YUAN-TING LIU, TSAI-TING WANG
Department of Biological Science and Technology, National Chiao Tung University, 75, Po-Ai Street, Hsin-Chu 300, Taiwan, R.O.C.

Received 15 June 2008; Accepted 1 August 2008

ABSTRACT: The oxidosqualene cyclases (EC 5.4.99-) constitute a family of enzymes that catalyze diverse cyclization/rearrangement reactions of (3*S*)-2,3-oxidosqualene into a distinct array of sterols and triterpenes. The relationship between the cyclization mechanism and the enzymatic structure is extremely complex and compelling. This review covers the historical achievements of biomimetic studies and current progress in structural biology, molecular genetics, and bioinformatics studies to elucidate the mechanistic and structure–function relationships of the *Saccharomyces cerevisiae* oxidosqualene-lanosterol cyclase-catalyzed cyclization/rearrangement reaction. © 2008 The Japan Chemical Journal Forum and Wiley Periodicals, Inc. Chem Rec 8: 302–325; 2008: Published online in Wiley InterScience (www.interscience.wiley.com) DOI 10.1002/tcr.20157

Key words: oxidosqualene cyclase; biomimetic; site-saturated mutagenesis; molecular evolution; protein engineering; protein plasticity

Introduction

Oxidosqualene cyclases catalyze the enzymatic conversion of an acyclic polyolefin substrate, (3*S*)-2,3-oxidosqualene (**OS**), into a vast skeletal diversity of polycyclic sterols and triterpenoids. In turn, the products serve as biosynthetic precursors for sterols, related membranous components, steroid hormones, and secondary metabolites. The enzyme exhibits product specificity in a species-dependent manner. Nearly 200 distinct triterpenoid skeletons, mainly tetracycles and pentacycles, have been isolated from various sources.[1,2] The diverse product profile is primarily controlled by the preorganized substrate conformation, regio- and stereocontrol of the ring skeleton, varied degrees of cyclization and rearrangement, and a final deprotonation step at different positions through abstraction of a proton or addition of water molecules.[3,4] Additional dimensions of product diversity come from the enzymatic oxidation or functional derivation with diverse auxiliary components such as sugars, amino acids, peptides, or fatty acids.[1] In fungi and mammals, oxidosqualene is solely transformed into a unique tetracyclic lanosterol, whereas a variety of polycyclic triterpene alcohols, including cycloartenol, lupeol, or β-amyrin, are produced in higher plants and algae. In lower plants and bacteria, squalene-hopene cyclase (SHC) converts the precursor of oxidosqualene, squalene, into pentacyclic hopene or hopanol, which acts as corresponding sterol surrogates of eukaryotic membranous triterpenoid lipid components (Scheme 1).

The intrinsic reaction complexity and product diversity of oxidosqualene cyclase-catalyzed biotransformation have made it one of the most exceptional biological reactions found in nature, and have fascinated both bioorganic chemists and biochemists alike for over half a century, especially on the study

▸ ***Correspondence to*:** Tung-Kung Wu; e-mail: tkwmll@mail.nctu.edu.tw

The Chemical Record, Vol. 8, 302–325 (2008)

of the enzyme-catalyzed cyclization/rearrangement reaction mechanism.[5,6] The proposed enzymatic mechanism of lanosterol synthesis involves a highly diverse and complex process of substrate prefolding, acid-catalyzed epoxide protonation, consecutive ring cyclization, hydride or methyl group rearrangement, and a final deprotonation step (Scheme 2). In addition, the studies of oxidosqualene cyclase-catalyzed reactions suggest that the cyclization and rearrangement sequences can break up to 16 bonds and form 16 new bonds (e.g., in the conversion of **OS** to friedelin) as well as generate compounds with up to 10 stereocenters in a single reaction (e.g., lupeol or taraxasterol).[7] The remarkable product specificity/diversity and stereos-pecificity is primarily controlled by the prefolded substrate conformation as well as the interactions between a series of discrete, conformationally rigid, partially cyclized carbocationic intermediates for deprotonation and the functional groups of the catalytic amino acid residues of the enzyme. For oxidosqualene-lanosterol cyclase (OSC or ERG7)- and oxidosqualene-cycloartenol synthase (CAS)-catalyzed cyclization/rearrangement reactions, the substrate enters the enzyme active site in a prefolded chair–boat–chair (C-B-C) conformation, initiates and propagates the cyclization via an oxirane ring protonation and cleavage, to form a tetracyclic protosteryl cation. This is followed by a series of 1,2-shifts of hydride and methyl groups to the lanosteryl C-8/C-9 cation. Lanosterol is formed through abstracting a proton from lanosteryl C-8 or C-9 cationic intermediate, whereas cycloartenol is produced by deprotonation from the C-19 position and forming a cyclopropyl ring. On the other hand, the formation of triterpene alcohols, such as pentacyclic β-amyrin and lupeol, catalyzed by β-amyrin synthase and lupeol synthase, respectively, proceeds similarly except that the **OS** is prefolded into a chair–chair–chair (C-C-C) substrate conformation, and proceeds with a cationic cyclization to a dammarenyl cation, which is followed by annulation of a fifth ring and/or hydride migration. A generally accepted mechanism for the formation of lanosterol

Tung-Kung Wu was born in 1963 in Taiwan. He received his M.S. degree from the Chemistry Department of National Taiwan University under the supervision of Professor Tahsin J. Chow in 1988. In 1996, he received his Ph.D. degree in Biophysics from the Johns Hopkins University under the supervision of Professor Craig A. Townsend. From 1996 to 1998, he worked as a postdoctoral research fellow at Stanford University under the supervision of Professor John H. Griffin. He was appointed assistant professor in the Department of Biological Science and Technology at the National Chiao Tung University in 1998, and was promoted to associate professor in 2004. His research interests include the interdisciplinary fields of organic chemistry, biochemistry, molecular biology, and genetics. His current research interests are mainly in the structure, function, mechanism, and biotechnological applications of oxidosqualene cyclases and molecular evolution of artificial enzymes for biosolar photovoltaic energy conversion. ■

Cheng-Hsiang Chang was born in Taichung County, Taiwan, in 1977. He received his B.S. degree from the Department of Chemistry at National Chiao Tung University in Hisnchu City, Taiwan, in 2000. He then started his graduate studies on oxidosqualene cyclase under the supervision of Professor Tung-Kung Wu in the Laboratory of Bioorganic Chemistry and Molecular Evolution at the Department of Biological Science and Technology in the same school. During the first year of his Ph.D. program, he studied the enzymology of oxidosqualene cyclase and, with his coworkers, established a purification procedure for it from crude tissue. He received his Ph.D. degree in Biological Science and Technology. His research focuses on the functional characterization of oxidosqualene cyclases via various experimental strategies including mutagenesis approaches, inhibition studies, and SELEX technology. He is also interested in the fields of molecular biology and bioorganic chemistry and their relevance to the structural–functional relationships of cyclase enzymes. ■

from oxidosqualene cyclase-catalyzed reactions is summarized in Scheme 2.

Early biomimetic studies on oxidosqualene cyclases, using radioisotope tracers and substrate analogs, have provided important mechanistic insights regarding steric and functional tolerance of the substrate within the enzyme, as well as the nature of the resulting products.[3,4] However, detailed structure–function relationships for how enzyme functional residues interact with substrates for preferentially promoting certain cyclization, rearrangement, or deprotonation modes, await protein–ligand complex structure determination, or molecular-genetic selection coupled with product isolation and characterization.

In this paper, we historically review achievements by biomimetic studies and emphasize the current progress with regard to the *Saccharomyces cerevisiae* oxidosqualene-lanosterol cyclase (*Sce*ERG7) enzyme. In this enzyme, site-directed and site-saturated mutagenesis coupled with genetic complementation and product characterization have been applied to identify catalytically important residues, to characterize the carbocationic intermediates involved in cyclization/rearrangement cascade and to elucidate the structure–function–reaction mechanism relationships. The goal of this report is to unravel the complexities of oxidosqualene cyclization/rearrangement cascade for rational design of cyclase inhibitors for hypocholesterolemic, antifungal, and phytotoxic drugs, and to illuminate the process whereby protein engineering can generate new cyclases with novel or altered activity.

The Mechanistic and Stereochemical Insights for Oxidosqualene Cyclization

Detailed mechanistic studies of oxidosqualene cyclization to form polycyclic products started with radioisotope tracer experiments performed by Woodward and Bloch in 1953, which demonstrated that cholesterol and lanosterol are derived from squalene via a course of cyclization, followed by rear-

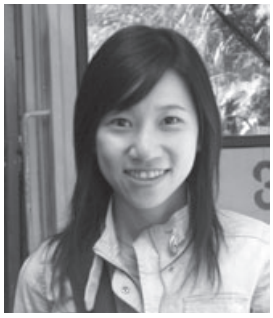

Yuan-Ting Liu was born in Kaohsiung County, Taiwan, in 1980. In 2002, she obtained her bachelor's degree from the Department of Medical Laboratory Science and Biotechnology at Central Taiwan University of Science and Technology, Taichung City, Taiwan. After that, she entered the Department of Biological Science and Technology at National Chiao Tung University and worked on her Ph.D. study in the field of molecular biology of oxidosqualene cyclase with Professor Tung-Kung Wu. Currently, she is investigating the relationships between enzymatic active site residues and cyclization mechanisms via mutagenesis approaches, and has produced several interesting findings. Her current research interests are the evolutionary divergence of cyclases from different species, especially the stereochemistry of enzymatic control, by using site-saturated mutagenesis and directed evolution. ■

Tsai-Ting Wang was born in Taichung County, Taiwan, in 1984. She obtained her B.S. degree from the Department of Chemistry at National Chung Hsing University, Taichung City, Taiwan, in 2006. Subsequently, she entered the Department of Biological Science and Technology at National Chiao Tung University to start her graduate studies on oxidosqualene cyclase in Professor Tung-Kung Wu's lab. Her current research focuses on investigating the precise molecular interactions involved in chair–boat bicyclic formation by using a site-saturated mutagenesis approach. ■

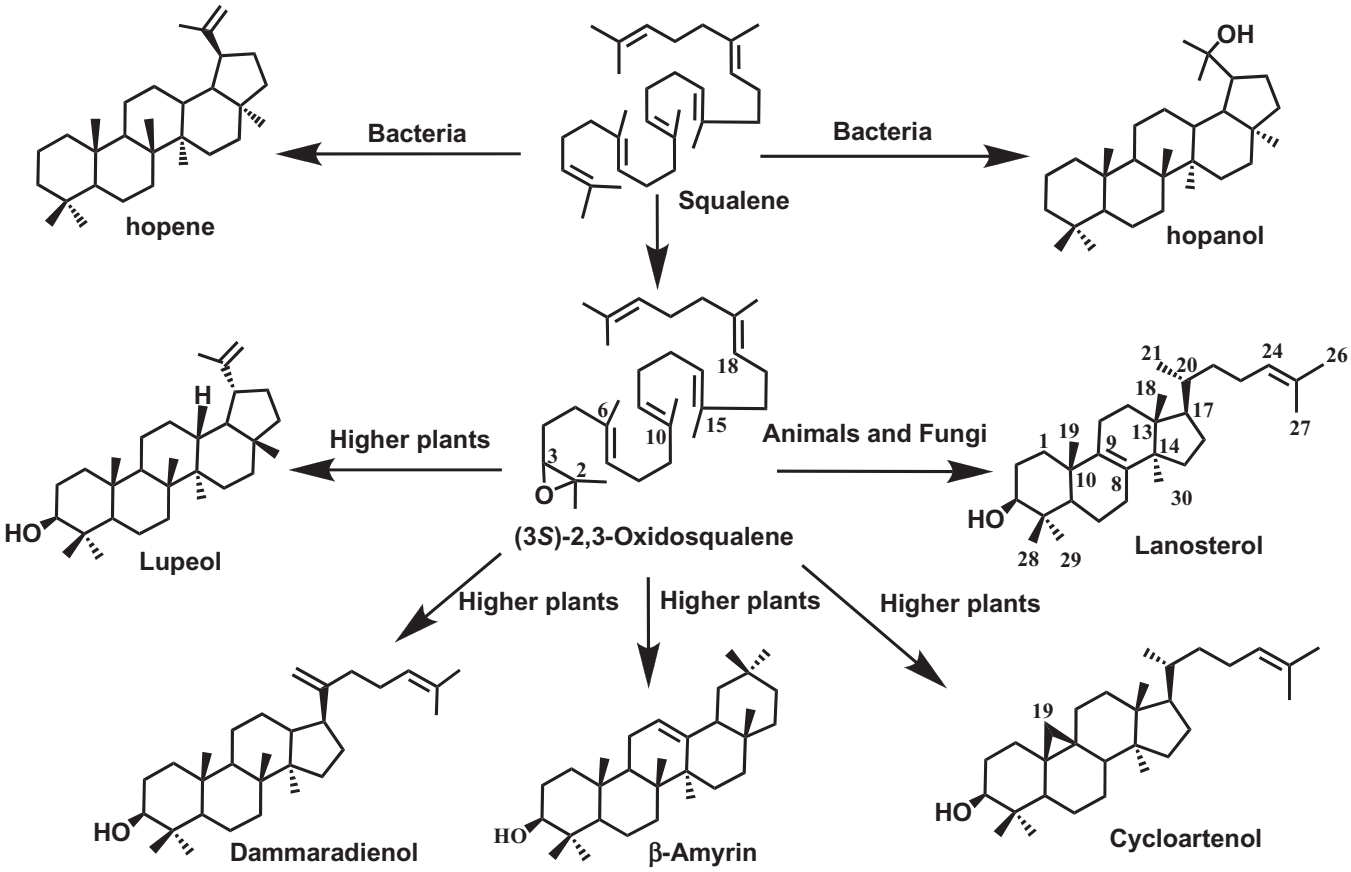

Scheme 1. Product diversity of (oxido)squalene cyclase in different species.

rangement.[8] In 1955, the groups of both Eschenmoser and Stork independently proposed a model for the stereochemical course of squalene cyclization and rearrangement.[5,6] The mechanism of two 1,2-methyl shifts rather than a single shift of a 1,3-methyl group as well as two 1,2-hydride shifts during lanosterol formation was demonstrated by Maudgal et al. in 1958 and Cornforth et al. in 1965, respectively.[9,10] In 1966, the groups of both Corey and van Tamelen showed that 2,3-oxidosqualene is far more efficiently incorporated in sterol synthesis than squalene, demonstrating the intermediacy of 2,3-oxidosqualene in lanosterol biosynthesis.[11–13] In parallel, van Tamelen also showed that nonenzymatic, chemical cyclization of 2,3-oxidosqualene resulted in truncated cyclization to yield a tricyclic compound, suggesting a direct enzymatic control in the formation of a six-membered C-ring.[14] In 1975, Barton et al. demonstrated that the (3*S*)- and not the (3*R*)-enantiomer of 2,3-oxidosqualene is incorporated into the formation of lanosterol by eukaryotic oxidosqualene cyclases.[15]

Enzymatic incubations of different chemically synthesized analogs or inhibitors have also provided valuable insight regarding the oxidosqualene cyclization mechanism. For example, a series of structural analogs have been utilized to elucidate the conformational requirement and molecular geometry of the substrate within enzyme active sites (Scheme 3).[16–27] A nonconcerted pathway, including a series of conformationally rigid and partially cyclized cationic intermediates, has been proposed for the cyclization cascade.[28,29] These chemical derivatives not only indicated the importance of internal methyl groups/unsaturated double bonds for the oxidosqualene cyclization, but also illustrated the enzymatic tolerance for the modification of oxidosqualene molecules. In addition, geometric isomers, *E*- or *Z*-form 2,3-oxidosqualene derivatives, have been used to evaluate the inhibitory effects on various oxidosqualene cyclases. The results showed that the natural substrate should be folded into the *E*-conformation, except for carbon-18, and cyclized via *all-trans* geometry for the cyclization reaction within the enzyme active site.[26,27,30] Moreover, anchimeric assistance from the neighboring double bond (C-6/C-7) has been proven for facilitating the initial protonation reaction as well as the A-ring formation.[31] In contrast, no enzymatic bicyclic triterpene alcohols derived from chair–boat (C-B)

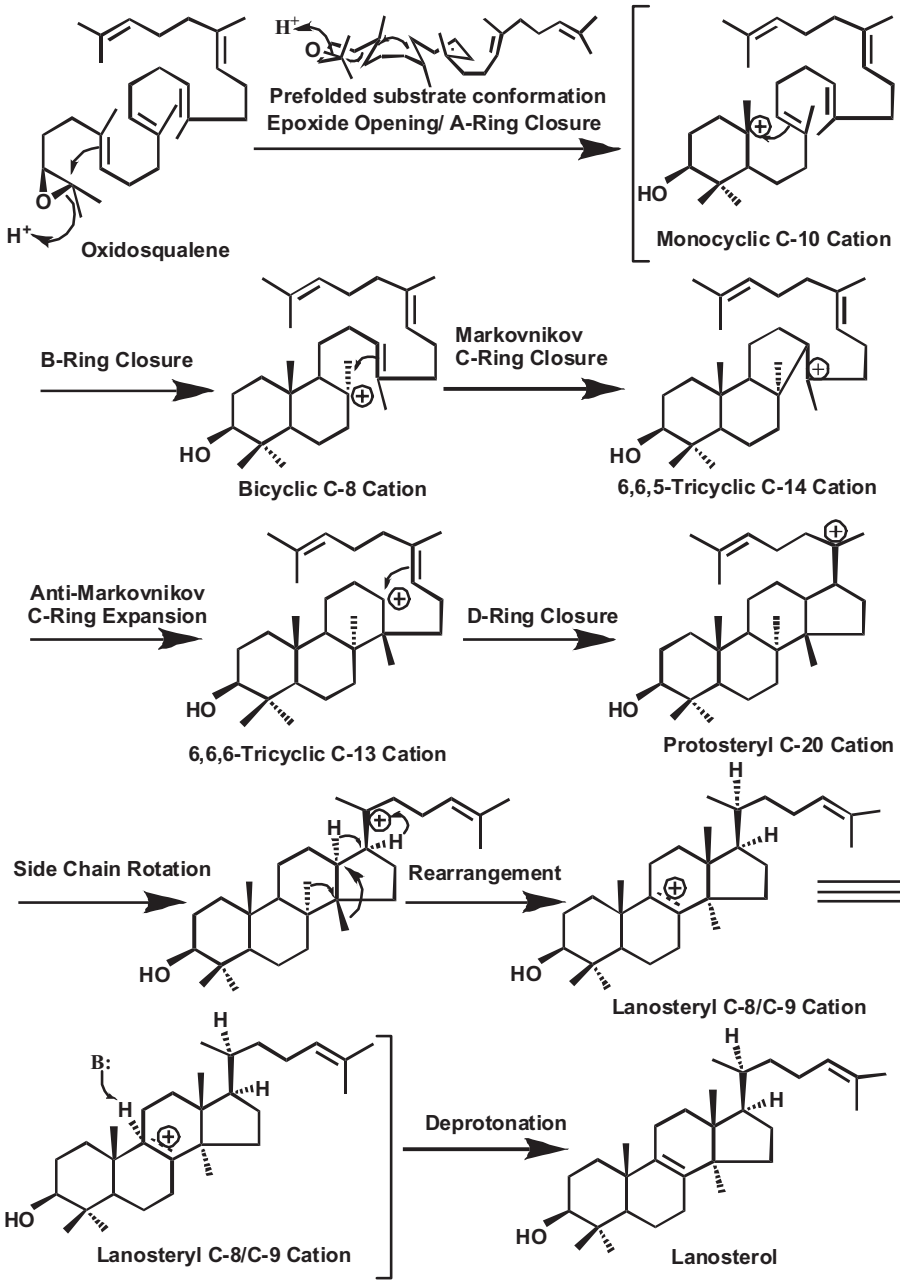

Scheme 2. Hypothesized cyclization/rearrangement mechanism for the conversion of oxidosqualene to lanosterol.

truncated bicyclic product could be isolated from natural sources, although B-ring boats are clearly present in triterpenoids with three or more rings. Importantly, the direct formation of a 6-6-6 tricyclic anti-Markovnikov ring closure was first against by Corey and co-workers in 1995.[32] The isolation of truncated product with a 6-6-5-4 tetracyclic scaffold from the enzymatic biotransformation of 20-oxa-2,3-oxidosqualene suggested that cyclization of **OS** to the tetracyclic protosteryl cation proceeds via a discrete tricyclic 6-6-5 Markovnikov carbocationic intermediate, which undergoes an anchimeric cyclopentylcarbinyl-cyclohexyl C-ring expansion and D-ring annulation, to generate the protosteryl cation. Many 6-6-5 tricycles occur in nature or have arisen from simple substrate analogs, whereas natural 6-6-6 triterpenes from (oxido)squalene are unknown, favorably supporting the intermediacy of the 6-6-5 tertiary cyclopentylcarbinyl carbocation.[2,33–37] Moreover,

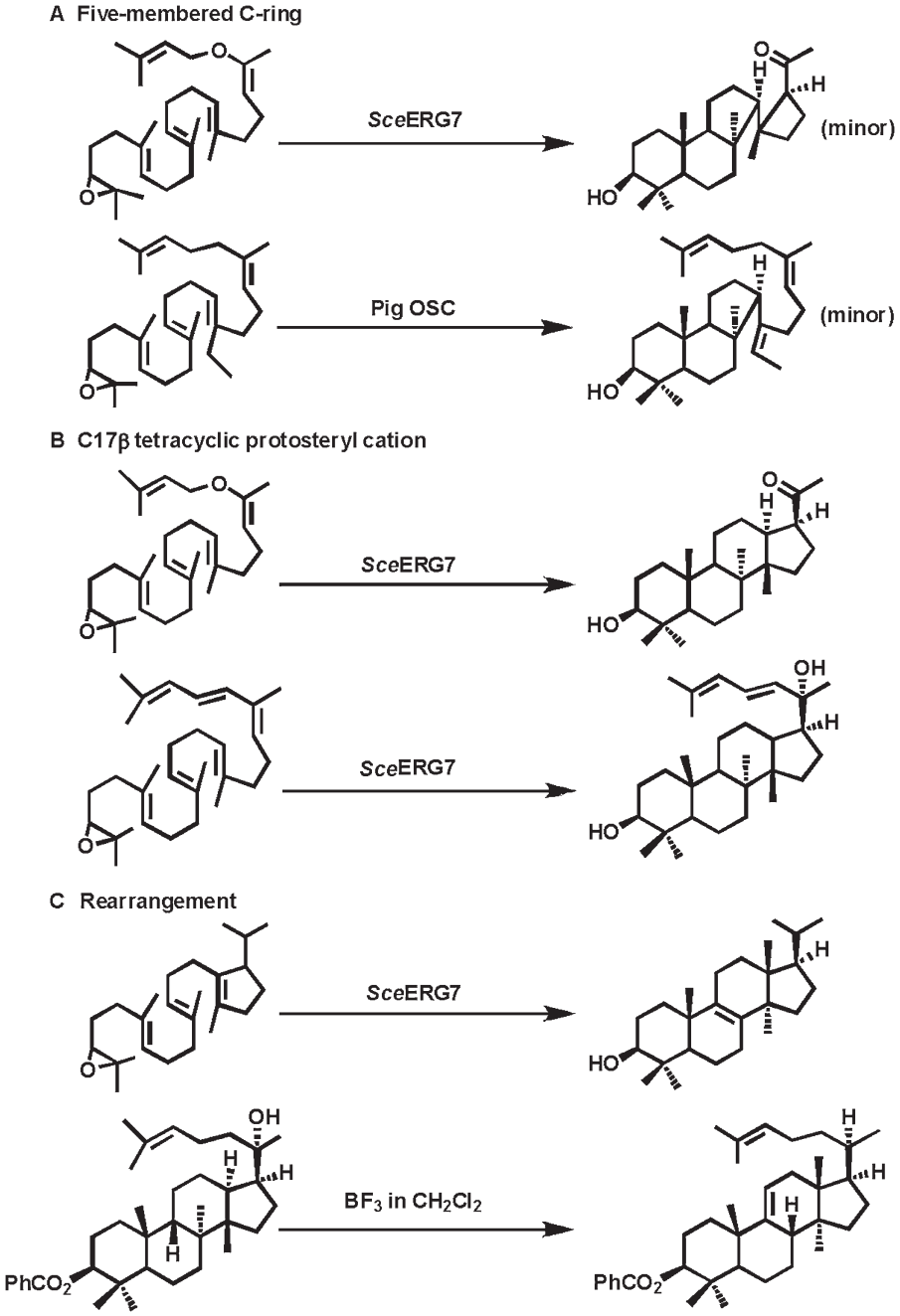

Scheme 3. Historic representatives of chemical studies of the respective cyclization steps.

the enzymatic conversion of 20-oxa-2,3-oxidosqualene and (20*E*)-20,21-dehydro-2,3-oxidosqualene into tetracyclic protosteryl derivatives with a 17β side-chain conformation excluded the previously hypothesized 17α side-chain conformation and facilitated an understanding of the natural *R*-form configuration at the C-20 position.[38,39] Following the formation of a 17β side chain, a smaller rotation angle (60°) of the side chain is required for producing the natural C-20*R* configuration. For the rearrangement steps, either enzymatic incubation of substrate analogs or nonenzymatic Lewis acids-catalyzed natural substrate cyclization produced products with spontaneous hydride or methyl group migrations.[14,34,40] Interestingly, the enzymatic active sites of oxidosqualene cyclases prevented early deprotonated truncation or nonspe-

cific water nucleophilic addition to generate biosynthetic products with high specificity and stereoselectivity. Scheme 3 shows representative observations of chemical studies on the respective stages of the cyclization processes.

Models for Cyclase Evolution and Biological Studies of Oxidosqualene-Lanosterol Cyclase

Although elegant biomimetic studies have provided important insights concerning the reaction mechanism, detailed mechanistic understanding of these biosynthetic processes had not been achieved, and there was a need in the field for direct examination of the cyclase enzymes. Evolutionary considerations regarding sterol biosynthesis had originally led Nes and then Ourisson et al. to propose a phylogenetic hypothesis for the cyclases. The extant cyclase enzymes could have evolved from a primitive cyclase through a process of gene duplication and divergence, and differences in product specificity could have arisen through mutations, which change the shape of the active site cavity and/or the positions of the crucial functional groups.[41–44] In parallel, Johnson and colleagues proposed a "cation-stabilizing auxiliary" model, in which a Lewis acid residue acts as the proton donor for the initiation of ring cyclization and axial negative point charge residues face toward the transition states or high-energy intermediates for cation stabilization.[45,46] Accordingly, the negative charge residues might lower the activation energy for the formation of the boat B-ring and/or the anti-Markovnikov closure of the C-ring. Many squalene cyclases and oxidosqualene cyclases, ranging from bacteria[47] to yeast,[48–52] mammals,[53–55] and plants,[56,57] were cloned and sequenced. Comparison of the sequence similarities among all the known cyclases has greatly facilitated the deduction of the putative active sites responsible for the cyclization, rearrangement, and deprotonation steps. In 1994, Poralla et al. noted an unusual abundance of aromatic amino acids in both SHCs and OSCs, and hypothesized a "Q-W" motif, where a 16-amino acid repeat might be involved in the binding and/or catalysis of the triterpenoid cyclases.[58,59] A DXDDTA motif of prokaryotic SHCs, which corresponds to the VXDCTA motif of eukaryotic OSCs, was also identified. Furthermore, there is evidence that different triterpenoid cyclases may have evolved from stepwise evolution of new motifs or inactivation of existing ones.[41–44] Alternatively, Shi et al. has proposed an "aromatic hypothesis" model where electron-rich aromatic side chains from Trp, Tyr, and perhaps Phe might play important roles in stabilizing protein structure or in generating, shepherding, and terminating electron-deficient intermediates or a transition state through polar–quadrupolar interactions between substrate and protein.[51] The stabilization of ground and transition states through cation–π interaction has been shown by Dougherty et al. in biomimetic model studies and applied to predict the involvement of aromatic side chains in receptors and enzymes.[60–63]

In 1997, Wendt et al. reported the X-ray analysis of *Alicyclobacillus acidocaldarius* squalene-hopene cyclase (*Aac*SHC), which is the first three-dimensional crystal structure among the many known triterpene synthases.[64–66] An X-ray structural examination revealed that the substrate analog binds to the enzyme's central cavity with a conformation very close to the *all-chair* conformation of the product hopene, and forms a salt bridge to Asp376 of *Aac*SHC. The enzymatic reaction is initiated by protonation of the double bond by the catalytic acid Asp376, which is hydrogen bonded to His451. After deprotonation, Asp376 is largely stabilized by a positively charged His451, which in turn is electrostatically stabilized by the water bridge to Tyr495-OH.[66] Following protonation, the cyclization reactions undergo only small conformational changes during the first four-ring formation.[67] The termination reaction was presumably presented by a polar amino acid (Glu45) associated with a water molecule for effectively abstracting the proton or hydroxylation of the cationic intermediate.[65–67] In parallel, several putative cation-stabilizing residues have been subjected to mutational studies to evaluate their importance in different stages of the squalene cyclization process.[4,36,65,66,68–75] Different truncated cyclization products, ranging from monocyclic to pentacyclic triterpenoids, have been obtained from point mutations of Trp169, Ile261, Gln262, Pro263, Trp312, Phe365, Asp377, Tyr420, Trp489, Gly600, Phe601, Phe605, Leu607, Tyr609, and Tyr612. The site-directed mutagenesis, substrate analogs on the catalytic mechanism, and substrate recognition by *Aac*SHC have been extensively reviewed by Hoshino and Sato in 2002.[75] However, molecular level differences between squalene cyclases and oxidosqualene cyclases mediate differences in the reaction mechanism, including the use of squalene and oxidosqualene as a substrate, the opposite substrate folding during B-ring formation, cyclohexyl D/E-ring formation, and absence of the rearrangement steps. Solely based on SHC, these differences all account for the elucidation of oxidosqualene cyclization to be a plausible but adventurous challenge.

On the other hand, catalytically or structurally important residues within oxidosqualene cyclases were identified via an affinity-labeling strategy of substrate analogs (Scheme 4).[76,77] For example, the DCTAE motif, a highly conserved region in cyclases, was specifically labeled with the first mechanism-based irreversible inhibitor, 29-methylidene-2,3-oxidosqualene (29-MOS), implicating the functional importance of this region in the oxidosqualene cyclization process.[53,78] The tritium-labeled 29-MOS was further used to identify the alkylated site (Asp456) of rat OSC.[76] Similar experimental results were observed in *Aac*SHC, suggesting the central influence of this region on cyclase activity.[68,79] In addition, three mechanistic inhibitors (6-desmethyl-2,3-oxidosqualene, 10-

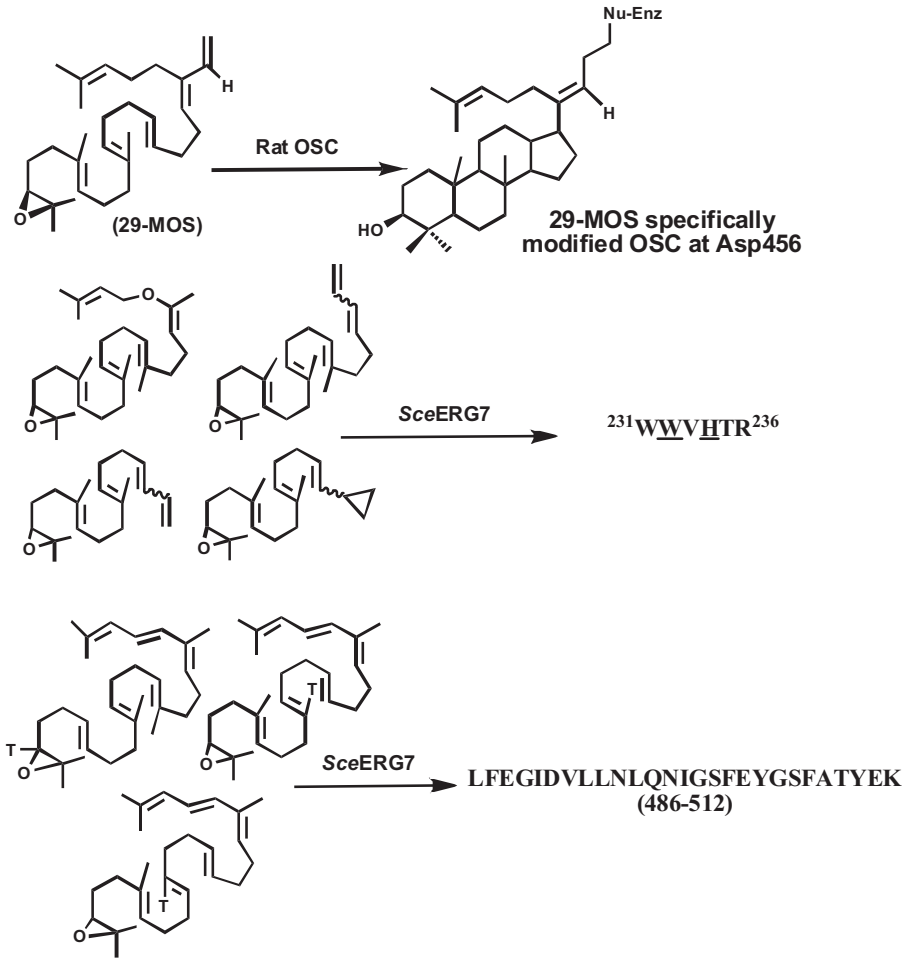

Scheme 4. Affinity-labeled cyclase fragment with respective mechanistic suicide inhibitors. Underlines indicate the exact attachment sites.

desmethyl-2,3-oxidosqualene, and 10,15-desdimethyl-2,3-oxidosqualene), which were expected to mimic monocyclic or bicyclic intermediates, specifically inactivated the enzyme with covalent attachment to the 486–512 segment of *S. cerevisiae* ERG7 (*Sce*ERG7) enzyme.[31,77] The 20-oxa-2,3-oxidosqualene and three other 2,3-oxidosqualene analogs, which mimic the cationic intermediate during D-ring formation, were found to covalently label *Sce*ERG7 within the fragment 231–236. In addition, site-directed mutagenesis analyses of 76 amino acid residues, which are highly conserved within various ERG7s, have revealed that Asp456, His146, and His234 are essential for catalytic activity.[31,77] The Asp456 and protonated His146 residue were implied as candidates in the activation of the oxirane function and enhancement of Asp456 acidity, respectively, to initiate cyclization. However, the precise functional role of these residues in controlling the cyclization process or whether there are more catalytically important amino acid residues involved in different stages of the complex cyclization/rearrangement cascade remains unclear. In contrast, no residues have ever been identified to facilitate the substrate-folding, cyclization, or rearrangement processes, either from experiments on mechanism-based inhibition or site-directed mutagenesis. Further validation of mechanistic hypothesis awaits direct structural determination of the cyclases to understand how enzymes preferentially promote certain cyclization, rearrangement, or deprotonation reactions over others, and control product structure.

A Crossroad Between Oxidosqualene-Lanosterol Cyclase and Oxidosqualene-Cycloartenol Synthase

Among all oxidosqualene cyclase-catalyzed reactions, both OSCs and CASs are the only two examples that prefolded the **OS** substrate into the energetically unfavorable C-B-C conformation, and then proceeded with similar cyclization and rearrangement reactions until lanosteryl C-8/C-9 cation. ERG7 abstracts a proton originally at C-9 or after a hydride shift from

C-9 to C-8 to generate lanosterol, whereas CAS forms a 9β,19-cyclopropyl ring through abstraction of the proton from C-19 to form cycloartenol. Despite the parallel repetitive cyclization/rearrangement mechanism, *Sce*ERG7 shows 40 and 37% sequence identity to that of human OSC (*Hsa*OSC) and *Arabidopsis thaliana* CAS (*Ath*CAS), respectively (Fig. 1). The highly parallel mechanism indicates that some common residues may be involved to direct the cyclization and rearrangement, whereas some residues that differ between these enzymes may impart the catalytic distinction for specific deprotonation or cyclopropyl ring formation.

Both Matsuda's group and our group have independently aimed at the identification of important amino acid residues that impart catalytic distinction between cycloartenol formation and lanosterol production (Scheme 5). Mutants from random mutagenesis libraries of CAS with altered cyclase product specificity to lanosterol production could easily be uncovered by their ability to genetically complement a yeast ERG7 mutant. Hart et al. first generated spontaneous *Ath*CAS mutants and performed sterol auxotrophy complementation experiments to select CAS mutants that could alter CAS function to OSC activity. An Ile481Val (I481V) mutation within the *Ath*CAS gene was identified for its ability to genetically complement a yeast ERG7 mutant.[80] The substitution of a *sec*-butyl side chain with an isopropyl side chain at the CAS 481 position enabled the enzyme to convert oxidosqualene into lanosterol, parkeol, and cycloartenol at a ratio of 25 : 21 : 54, indicating a steric effect in broadening the product profile from cycloartenol alone to a mixture of lanosterol, parkeol, and cycloartenol. Further steric changes at this position with Phe, Leu, Ala, and Gly showed that the increased steric bulk of Phe resulted in an inactive mutation, whereas a similar size but different shape of Leu altered the product profile to a different deprotonation.[81] Reducing the size of the substituting group not only compromised cycloartenol biosynthesis to lanosterol and parkeol production, but also facilitated premature deprotonation, either through enlarging the active site cavity for an alternative folding pattern or by shifting the alignment of the olefin around the A- or B-ring. Multiple sequence alignments among various ERG7s and CASs also revealed differences in conserved residues where all known CASs had a conserved Ile at this position and ERG7s, a conserved Val, indicating that this position is at least partly responsible for the catalytic distinction between deprotonation and cyclopropyl ring formation. Mutated enzymes that formed altered deprotonation or truncated cyclization may have less sterically bulky groups at this position.

Herrera and coworkers then performed a search for similar conserved patterns between CASs and ERG7s. From a series of conserved residues including Tyr410, Gly488, Phe717, and Met731 of CAS, a Tyr410Thr (Y410T) mutation was identified to alter catalysis, and produced lanosterol, parkeol, and 9β-lanosta-7,24-dien-3β-ol at a ratio of 65 : 2 : 33.[82] The generation of by-products from the Y410T mutation suggested that additional mutations are necessary to specifically convert CAS into an accurate OSC. A CAS$^{Y410T/I481V}$ double mutant was then constructed and found to have a synergistic effect of lanosterol production, but still with the formation of 9β-lanosta-7,24-dien-3β-ol. These results indicated that a third residue mutation, in addition to I481V and Y410T, is necessary for accurate construction of the OSC deprotonation motif from the CAS cyclopropyl ring formation motif.

In early 2002, we performed random mutagenesis and *in vivo* selection experiments to identify changes in the *Ath*CAS that impart this enzyme with ERG7 activity.[83] Two independent approaches, one with chemical mutagenesis by hydroxylamine, and the other utilizing the *Ep. coli* XL1-Red mutator strain deficient in DNA repair pathway, were undertaken to generate random mutations in the *Ath*CAS gene. The *Ath*CAS mutated libraries were heterologously expressed within an ERG7 knockout yeast haploid strain, which bears a genomic *erg7*-disrupted gene and complements the cyclase deficiency by the wild-type ERG7 gene carried on a plasmid or from a mutated *cas* gene that can alter CAS function into OSC activity. Five unique product specificity-altering point mutations, including Tyr410Cys (Y410C), Ala469Val (A469V), His477Tyr (H477Y), Ile481Thr (I481T), and Tyr532His (Y532H), were capable of complementing the ERG7-deficient knockout yeast strain. Among the mutations, three that have been isolated occur at positions not previously known to have an impact on product selectivity in the oxidosqualene cyclase family. Interestingly, three of the mutations (A469V, H477Y, and I481T) occur proximal to the putative active site Asp483 in the *N*-terminal direction, while two more mutations locate somewhat more distal in the *N*-terminal (Y410C) and *C*-terminal (Y532H) directions. In addition to lanosterol, which was identified in all of the mutants, a monocyclic achilleol A was isolated from the *Ath*CAS A469V, I481T, and Y532H mutants. The structural homology model of CAS, using the X-ray structure of SHC from *A. acidocaldarius*, showed that Tyr410, Ile481, and Tyr532 were located within the active site cavity of the cycloartenol synthase, whereas Ala469 and His477 appeared to lie outside the enzyme active site. Ala469 and His477 may be the nearest neighbors to the active site residues, and thereby provide indirect influence on the active site structure.

Using the *Dictyostelium discoideum* oxidosqualene-cycloartenol synthase (*Ddi*CAS1), Meyer et al. iteratively performed random mutagenesis and a selection process. These screens resulted in identification of Tyr363Cys, Phe424Ser, Ser434Pro, and Tyr481His mutations, each of which allowed genetic complementation of the yeast ERG7 mutant.[84] The corresponding positions within *Ath*CAS [*Ath*CAS Tyr410Cys (Y410C), Phe472Ser (F472S), Ser482Pro (S482P), and

Fig. 1. Representative multiple sequence alignment of squalene and oxidosqualene cyclases. Shown are oxidosqualene-lanosterol cyclases from *Homo sapiens* (*Hsa*OSC), *Saccharomyces cerevisiae* (*Sce*ERG7), oxidosqualene-cycloartenol synthase from *Arabidopsis thaliana* (*Ath*CAS), and squalene-hopene cyclase from *Alicyclobacillus acidocaldarius* (*Aac*SHC).

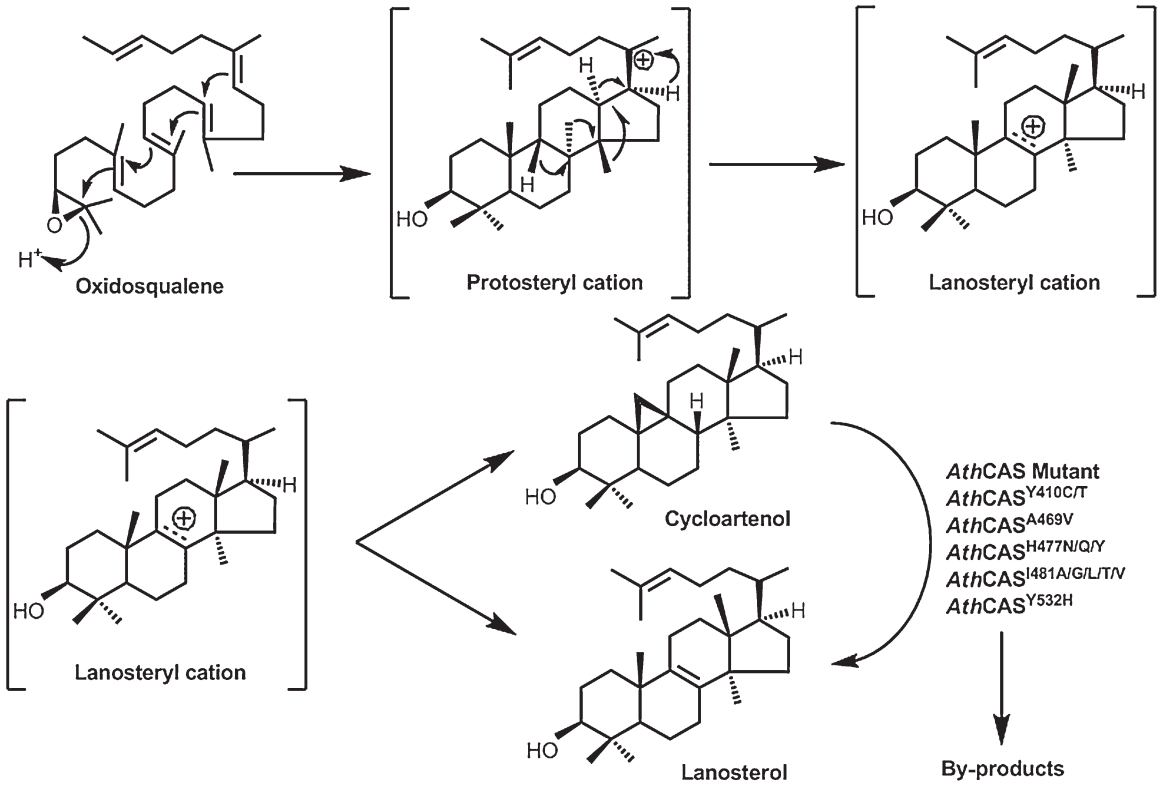

Scheme 5. *Ath*CAS mutants changed product specificity from the cycloartenol formation to the lanosterol production.

Tyr532His (Y532H) mutations] were then site-specific mutated for accurate comparison of mutational effects on product specificity. Among them, the *Ath*CAS^{Y410C} mutant produced lanosterol, 9β-lanosta-7,24-dien-3β-ol, and achilleol A at a 75 : 24 : 1 ratio, where the product profile resembles that of the Y410T mutation with a structural similarity between Cys and Thr.[84] The Y532H mutation produced lanosterol, parkeol, and achilleol A (45 : 31 : 24). Multiple sequence analyses showed that Tyr at this position is conserved in all known examples of oxidosqualene cyclases that adopt the C-B-C prefolded substrate conformation, whereas a Trp residue is strictly maintained at the corresponding position for a substrate prefolded into the C-C-C conformation. Observation of the Tyr residue in both ERG7s and CASs excluded the functional role of this residue in the catalytic distinction between cycloartenol cyclopropyl ring formation and the lanosterol deprotonation step. The isolation of a monocyclic achilleol A from the CAS^{Y532H} mutant indicates a functional role of Tyr532 in cyclization.[83,84]

In late 2002, Segura et al. pursued a different cycle of random mutagenesis and screening and identified a His477Asn (H477N) mutation, which converted oxidosqualene to 88% lanosterol and 12% parkeol.[85] The observation of this residue in the known CAS, but not in ERG7, and the observed product profile led Segura et al. to suggest that this residue might play an essential role in promoting cyclopropyl ring formation. Recently, CAS Y410T, H477N or H477Q, and/or I481V mutations were combined by Lodeiro and coworkers to more accurately produce lanosterol.[86] The CAS$^{H477N/I481V}$ double mutant was observed to be the most perfect example of an enzyme mutated to produce lanosterol with 99% accuracy, while the CAS$^{Y410T/H477N/I481V}$ triple mutant still yielded 22% 9β-lanosta-7,24-dien-3β-ol.[86] Computer models showed that the H477N/I481V double mutant relocated polarity to a position more favorable for lanosterol formation. The decreased sterics allowed the intermediate to rotate and moved the lanosteryl C-8/C-9 cation toward the base. In contrast, introduction of the third Y410T mutation into the H477N/I481V double mutant increased the distance and reduced the interactions between H477N and Y410T, and therefore did not influence catalysis.[86]

Structural Determination of Human Oxidosqualene-Lanosterol Cyclase

In 2004, the long-awaited X-ray structure of human OSC, which is in complex with lanosterol, was solved by Thoma and

co-workers.[87] The crystallographic analysis of human OSC provided a three-dimensional framework for enzymatic **OS** cyclization. The human OSC–lanosterol complex structure showed that a hydrogen bond formed between the lanosterol 3-hydroxyl group and the catalytic Asp455 (corresponds to Asp456 of *Sce*ERG7). It putatively constitutes the polar cap of the mainly hydrophobic cavity, confirming the proposed role of Asp455 as the general acid that initiates the cyclization reaction through protonating the epoxide group of prefolded **OS**. The required increased acidity of Asp455 in human OSC was provided by the formation of additional hydrogen bonds between Asp455 and Cys456 as well as with Cys533. After completion of the catalytic cycle, the deprotonated Asp455 can either be reprotonated from the bulk solvent through a chain of water molecules and the carboxylate group of Glu459 or by shifting the proton from the final deprotonation step back to Asp455. The tetracyclic ring-forming process proceeds via cation–π interactions between the π-electrons of the conserved aromatic side chain of Trp, Tyr, or Phe and the partially cyclized carbocationic intermediates. The conserved aromatic side chains of Phe444, Tyr503, and Trp581 are appropriately positioned and orientated to stabilize the monocyclic C-10 and bicyclic C-8 cations (lanosterol numbering), respectively. The Tyr98 in human OSC is well located spatially to enforce the energetically unfavorable *boat* conformation of **OS** for lanosterol B-ring formation by pushing the methyl group at C-8 below the molecular plane. For the C-ring formation, His232 and Phe696 residues are positioned to stabilize the C-13 (lanosterol numbering) anti-Markovnikov secondary cation through cation–π interactions. In contrast to the presence of aromatic residues Trp169 and Phe605 in *Aac*SHC, which stabilize the 6,6,6,5-fused tetracyclic secondary cation for hopene E-ring formation, no apparent aromatic residue could be identified at the corresponding position to stabilize the protosteryl C-20 cation. In human OSC, these positions are replaced with His232 and Cys700, respectively. The tetracyclic protosteryl cation then undergoes a series of 1,2-hydride and methyl group rearrangements to form the lanosteryl C-8/C-9 cation. Rearrangement reactions were suggested as being driven by a higher π-electron density gradient, at different active site regions, or by only a minimal assistance from the enzyme.[4,87–89] In addition, premature termination during the rearrangement steps by the nucleophilic addition of water molecules is avoided by the predominantly hydrophobic nature of the active site cavity. Final deprotonation occurs through abstracting a proton, either at the original C-9 site or after a hydride shift from C-9 to C-8, to form lanosterol. His232 in human OSC was also suggested to act as a base that abstracts the proton from the lanosteryl C-8/C-9 cation to form lanosterol.[77,90] Alternatively, the hydroxyl group of Tyr503 residue might also function for the final deprotonation via a hydrogen-bonding network to the Nε2 of the His232 imidazole group.[87] Interestingly, the X-ray structure of the human OSC complexed with the potential anticholesteremic drug Ro48-8071, revealing a different binding conformation from that of the *Aac*SHC Ro48-8071 complex, in which the basic nitrogen atom forms a charged hydrogen bond with the catalytic Asp455 that directs both oxygen atoms toward the active site cavity. The charged amino group is also stabilized through cation–π interactions with several aromatic residues.[87]

Although the human OSC crystal structure has provided valuable insights for understanding the OSC-catalyzed cyclization/rearrangement cascade, many fundamental questions around the complex reactions remain unanswered. For example, it would be of interest to know the relationships between the cyclization mechanism and the low sequence identity of the encoded active site structures of various OSC enzymes. In addition, how does the substrate **OS** fold into the energetically unfavorable C-B-C conformation in lanosterol and cycloartenol formation, but induce a C-C-C conformation in β-amyrin and lupeol production? Furthermore, how is product specificity from various species determined from subtle changes in the active site structure? Finally, does the formation of C and D rings proceed via an anchimeric cyclopentylcarbinyl-cyclohexyl C-ring expansion and D-ring annulation or through asynchronous concerted cyclization from the A/B bicyclic cation to D-ring formation? Clarification of the aforementioned questions awaits either additional X-ray structure determination of cyclases from other species or functional identification of the active site residues coupled with product isolation and characterization.

Site-Saturated Mutagenesis and Homology Modeling to Study *S. cerevisiae* Oxidosqualene-Lanosterol Cyclase

The highly parallel mechanisms by which OSC and CAS enzymes proceed, the clustering of product altering mutations in specific regions of CAS, and the evidence obtained from polyterpenoid fossils indicated that various skeletons of sterols and triterpenoids could be obtained by slightly altering the active site structure or subtly repositioning key amino acid side chains or domains within the enzyme. These observations led to a speculation that CAS-mutated regions might also be crucial in other cyclases in determining the cyclization/rearrangement cascade or product profiles. We therefore set up a series of site-directed and site-saturated mutagenesis experiments to investigate the corresponding regions in *Sce*ERG7 to evaluate the effects on the cyclization/rearrangement mechanism and product specificity/diversity. To elucidate the evolutionary pattern of catalytic relevance within these regions, the alanine-scanning method was used to mutate the corresponding or neighboring residues in *Sce*ERG7, which are parallel to

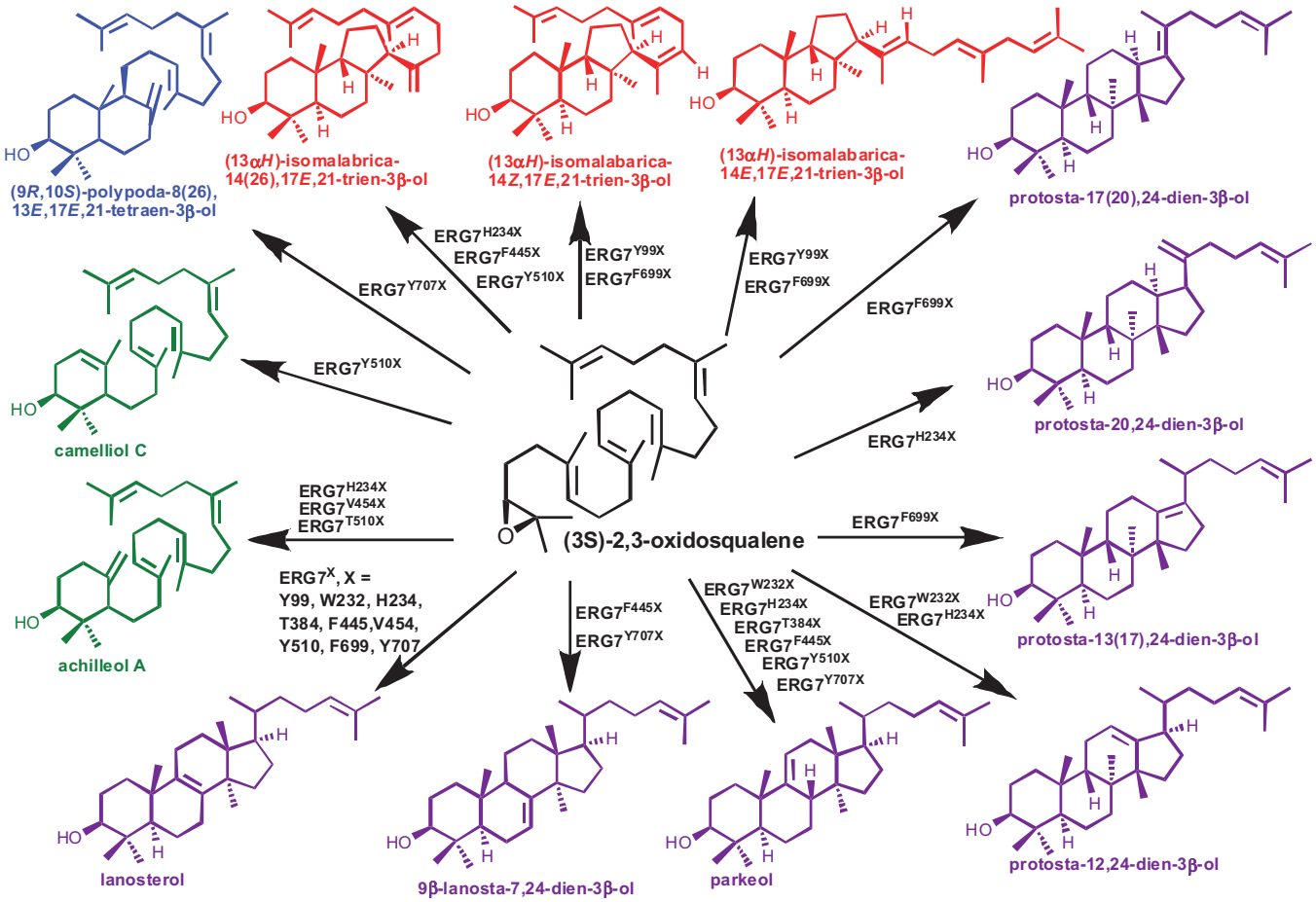

Fig. 2. Isolated products from various *Saccharomyces cerevisiae* ERG7^{X} mutation studies.

the CAS mutations previously identified. Next, highly conserved or conservatively different residues identified from multiple sequence alignments of known triterpene synthases, functioning as OSCs, CASs, α- and β-amyrin synthases, and lupeol synthases, from various species, were also subjected to mutagenesis to determine the functional role of these residues in catalysis or product specificity. Site-saturated mutagenesis, which replaces the target residue with each of the other proteinogenic amino acids, was then applied to obtain a detailed understanding of the effects, either steric or electrostatic, of other amino acid residues in the corresponding position (Fig. 2).

The catalytically important *Ath*CAS Tyr532 residue corresponds to Tyr510 in the *Sce*ERG7 (*Sce*ERG7^{Y510}). To determine whether the corresponding or neighboring residues within *Sce*ERG7 are important for controlling product specificity, the amino acid residues positioned from 509 to 513 of *Sce*ERG7 were subjected to alanine-scanning mutagenesis. The *Sce*ERG7 Tyr510 position was previously mutated to Phe and showed viability when transformed into an ergosterol-free medium, but no product isolation and characterization was performed.[77] In addition, Tyr510 of ERG7 was also mutated to Trp and Lys, due to the observation that this residue is conservatively different in cyclases from the C-B-C and C-C-C substrate conformations and a different electrostatic substitution might affect cyclase function. As expected, the *Sce*ERG7 ^{509}TYEKI^{513} alanine-scanning mutants were active, whereas the Tyr510Lys (Y510K) and Tyr510Trp (Y510W) mutants were inactive. Product isolation and characterization of the Tyr510Ala (Y510A) mutant showed that the mutant produces achilleol A, lanosterol, and parkeol in a 27:39:34 ratio. Alternatively, the Y510K and Y510W mutants make achilleol A and camelliol A in ratios of 86:14 and 96:4, respectively. These results indicated that this residue might influence the monocyclic to tetracyclic formation and stabilize the lanosteryl C-8/C-9 cation for deprotonation.

We then investigated the amino acid residues putatively involved in differentiating the C-B-C and C-C-C conforma-

tions, in stabilizing carbocationic cyclization/rearrangement intermediates or in defining the termination position. His234 of *Sce*ERG7 (corresponds to His232 of human OSC) was of particular interest. As previously described, some studies suggested that this residue is the catalytic base, while others suggested that it acts to stabilize the tricyclic reaction intermediates.[4,77,87,90,91] The same residue was also suggested as influencing deprotonation via a hydrogen-bonding network to the hydroxyl group of Tyr510 of *Sce*ERG7. Both CASs and OSCs have a His residue at the corresponding position, while β-amyrin synthase and lupeol synthase both have a Tyr residue. The corresponding residue in the related *Aac*SHC is Trp169 residue. In addition, the bacterial SHC mutations at the Trp169 position led to the production of several abortive cyclization products, indicating the stabilization of His234 for the protosteryl C-20 cation in *Sce*ERG7, rather than acting as a catalytic base.[69] We thus performed *Sce*ERG7^{H234X} site-saturated mutagenesis experiments to investigate the effects of substitutions of other amino acid residues on the catalytic activity and product profile of the cyclase.[92,93] Three novel intermediates, a 6,6,5-fused *trans-syn-trans* tricyclic (13α*H*)-isomalabarica-14(26),17*E*,21-trien-3β-ol, a 6,6,6,5-fused tetracyclic protosta-20,24-dien-3β-ol, and a truncated rearranged 6,6,6,5-fused tetracyclic protosta-12,24-dien-3β-ol, in addition to monocyclic achilleol A, altered deprotonated parkeol, and lanosterol, were isolated from the His234 site-saturated mutants. Notably, this is the long sought-after mechanistic evidence for the formation of the C-B 6-6-5 tricyclic Markovnikov cation, 6-6-6-5 tetracyclic protosteryl cation, and the hydride-rearranged lanosteryl C-13 cation, respectively, during the cyclization/rearrangement cascade. In addition, the *Sce*ERG7 His234 to Ser and Thr mutations showed a complete change in product specificity from lanosterol formation to protosta-12,24-dien-3β-ol and parkeol production, respectively. These results directly supported the proposed mechanism on various cationic intermediates, the steric or electrostatic interactions between the His234 residue and the cationic intermediates, as well as the catalytic plasticity of *Sce*ERG7.

Detailed investigation of the steric or electrostatic effects on the intrinsic His234:Tyr510 hydrogen-bonding network for product profiles arose from the work coming from Matsuda's and our laboratory. Further site-directed mutagenesis of Tyr510 of *Sce*ERG7, performed by Lodeiro and coworkers, resulted in the formation of monocyclic, tricyclic, and tetracyclic byproducts.[94] The substitution of Tyr510 with Phe produces the tricyclic (13α*H*)-isomalabarica-14(26),17*E*,21-trien-3β-ol in addition to lanosterol, while the Y510H and Y510A mutants afford a mixture of the monocyclic achilleol A and parkeol. Recently, we constructed the *Sce*ERG7^{Y510X} site-saturated and three *Sce*ERG7 double mutants: His234Trp/Tyr510Trp (H234W/Y510W), His234Trp/Tyr510Val (H234W/Y510V), and His234Tyr/Tyr510Ala (H234Y/Y510A).[95] The *Sce*ERG7$^{H234W/Y510V}$ produced achilleol A, (13α*H*)-isomalabarica-14(26),17*E*,21-trien-3β-ol, and lanosterol at a 2 : 8 : 90 ratio. Alternatively, the *Sce*ERG7$^{H234W/Y510W}$ and *Sce*ERG7$^{H234Y/Y510A}$ mutants made achilleol A and lanosterol, respectively. The polycyclic products were isolated from the smaller group substitution of Tyr510 in either the H234W/Y510V or H234Y/Y510A mutants. This indicated the catalytic importance of His234 for the stabilization of the tricyclic C-14 and the tetracyclic C-20 protosteryl cations, whereas the bulky substitution at Tyr510 with Trp might interfere with the progression of cyclization beyond the monocyclic stage and result in high ratios of the monocyclic cyclization product, achilleol A. These experiments also illustrate how subtle changes in the *Sce*ERG7^{H234} catalytic environment have steric or electrostatic effects on the intrinsic His234:Tyr510 hydrogen-bonding network to alter product profiles.

We iteratively performed alanine-scanning mutagenesis on a series of amino acid residues, the sequence ^{441}GAWGFSTKTQGYT^{453} within the upstream region of the putative active site residue Asp456 of *Sce*ERG7. Based on this, a high frequency of residues within this region of *Ath*CAS was observed in altering CAS activity into OSC function.[83] Three alanine substitutions, Trp443Ala (W443A), Phe445A (F445A), and Lys448Ala (K448A), which failed to complement the cyclase deficiency, were identified. Gas chromatography analyses showed that the ERG7^{W443A} mutant makes achilleol A and camelliol C at a ratio of 68 : 32.[96] Further genetic selection results of the site-saturated mutagenesis of Trp443 with 18 other amino acids showed that only six mutations, including Trp443Ala, Trp443Leu, Trp443His, Trp443Cys, Trp443Met, and Trp443Phe, allowed for ergosterol-independent growth and yielded lanosterol as the sole product. Of the rest, which were all inactive mutations, only Trp443Lys produced monocyclic achilleol A and camelliol C at a ratio of 56 : 44. These results indicated that Trp443 might play a role in influencing substrate binding, stabilizing the expoxide protonation, and inducing A-ring formation via the stabilization of the monocyclic C-10 cation. Therefore, substitutions at the Trp443 position either completely abolished the cyclization, halted the cyclization reaction at the monocyclic stage, or there was no effect on the cyclization cascade and produced lanosterol as an end product. In parallel, Phe445 was also subjected to site-saturated mutagenesis to investigate the effects of substitutions of this residue in terms of catalysis and product specificity. Interestingly, polar group (Cys, Met, Asn, Thr, or Asp) substitution of Phe445 resulted in the production of tricyclic (13α*H*)-isomalabarica-14(26),17*E*,21-trien-3β-ol, 9β-lanosta-7,24-dien-3β-ol, parkeol, and lanosterol. These results suggested a catalytic role for Phe445 in *Sce*ERG7 catalysis that could affect cation stabilization at both the C-14 position for tricyclic products and position C-8/C-9 for final deproton-

ation products. Furthermore, substitutions of Phe445 with polar amino acids complemented cyclase deficiency but resulted in isolation of tricyclic and altered deprotonation products. This supports Johnson and coworkers' model that cation-π interactions, between a carbocationic intermediate and an enzyme, could be replaced by an electrostatic or polar amino acid of similar size to stabilize the cationic intermediates.[45,46] However, the modified electrostatic or polar interactions might slightly retard the folding of the D-ring and allow for truncated deprotonation but with product differentiation. In contrast, nonpolar hydrophobic side-chain substitutions at this position might disrupt either the cation–π or electrostatic interactions in the active site cavity compared with those of the wild-type enzyme.

It has been suggested that rearrangement steps during the oxidosqualene cyclase-catalyzed reaction are driven by either a π-electron density gradient, at different active site regions, or with only a minimal assistance from the enzyme.[4,87–89] Although a truncated rearranged product, protosta-12,24-dien-3β-ol, has been characterized from several *Sce*ERG7 His234 mutants, possible involvement of other amino acid residues in the rearrangement process could not be excluded. Aromatic amino acid residues with a consensus sequence among various oxidosqualene cyclases and spatially located between the protosteryl C-20 and lanosteryl C-8/C-9 position were of particular interest for this investigation. The assumption was that the higher the π-electron density in different active site regions would drive a rearrangement process, and their intrinsic reactivity would form cation–π interactions to carbocationic intermediates. Among the various aromatic residues of ERG7 under investigation, Trp232 is of particular interest. Trp232 is highly conserved in OSC, CAS, and β-amyrin synthase, but instead substituted by either Leu or Gly within lupeol synthase and SHC. Although site-directed mutagenesis of Trp232 with Ala, Gly, and Phe showed viability in genetic complementation experiments, substrate analog experiments showed that this residue was chemically inactivated by 20-oxa-2,3-oxidosqualene.[31,77] Moreover, a structural model of *Sce*ERG7 suggested a contribution of higher π-electron density near the C-12 position of lanosterol. Thus, the functional role of Trp232 was subjected to site-saturated mutagenesis and product characterization.[97] Interestingly, almost all of the Trp232 mutants were viable for genetic complementation assay and produced an identical product profile that included protosta-12,24-dien-3β-ol, parkeol, and lanosterol, but with varying product proportions. These results suggested a catalytic role for Trp232 in ERG7 that can influence both the rearrangement process and deprotonation position but is not involved in tetracyclic ring formation.

We then investigated the *Sce*ERG7 Tyr99 residue that corresponds to the catalytically important human OSC Tyr98 residue.[96] The human OSC Tyr98 residue was thought to be spatially positioned to enforce the energetically unfavorable boat conformation of lanosterol B-ring formation by pushing the methyl group at C-8 below the molecular plane. An apparent structural discrepancy with a one-residue insertion above and a one-residue deletion below the molecular plane was noted within the human OSC but absent in the bacterial SHC. However, although Tyr99 of *Sce*ERG7 is highly conserved in both the OSC and CAS, different substitutions were noticed for β-amyrin synthase and lupeol synthase. Furthermore, sequence alignment revealed that a one-residue insertion proximal to the Tyr99 position of *Sce*ERG7 was observed specifically for OSCs from *S. cerevisiae*, *Trypanosoma brucei*, and *Trypanosoma cruzi* but not for mammalian OSCs (data not shown). These observations suggested a possible different functional role for the Tyr99 residue of *Sce*ERG7 than that observed for the human OSC. The *Sce*ERG7 Tyr99 was treated to produce site-saturated mutations, and the mutant products were isolated and characterized. Interestingly, two tricyclic intermediates, (13α*H*)-isomalabarica-14*Z*,17*E*,21-trien-3β-ol and (13α*H*)-isomalabarica-14*E*, 17*E*,21-trien-3β-ol, in addition to lanosterol, were isolated from the $ERG7^{Y99X}$ mutants.[96] The data suggested that the Tyr99 residue in ERG7 might be involved in both the Markovnikov tricyclic C-14 cation stabilization, affecting the stereochemistry of the protons at the C-15 position for subsequent deprotonation, but it does not enforce the boat conformation for lanosterol B-ring formation.

Thoma et al. have previously proposed, from the human OSC X-ray structure, that His232 and Phe696 (which correspond to His234 and Phe699 of *Sce*ERG7, respectively) were positioned near the C-13/C-20 positions of lanosterol and for π–cation interaction with the C-13 anti-Markovnikov tricyclic cation, which is created from the Markovnikov tricyclic C-14 cation (lanosterol numbering).[87] As previously described, His234 of ERG7 was suggested to play a key role in stabilizing various carbocation intermediates and guiding deprotonation reactions.[92,93] The corresponding residue of Phe699 of *Sce*ERG7 in the related *Aac*SHC enzyme is Phe601. Numerous 6,6,5-tricyclic by-products were isolated from the Phe601Ala replacement of *Aac*SHC.[36] The structural model of ERG7 suggested that the Phe699 has the π-electron density positioned below the molecular plane of the substrate as well as near the D-ring and the exocyclic terminal hydrocarbon side-chain junction, and might affect either the H-17α→20α or the H-13α→17α, 1,2-hydride shift. We suspected that substitution of Phe699 with hydrophilic polar uncharged residues might disrupt the predominantly hydrophobic nature of the active site cavity resulting in an equilibrium shift from protosteryl cation to lanosteryl C-8/C-9 cation for lanosterol formation. It could also act as a basic residue to accept a proton in the specific deprotonation of the lanosteryl C-17 cation that terminates catalysis. Thus, Phe699 was mutated to polar uncharged amino

acid residues, such as Ser, Thr, Cys, Gln, and Tyr, to investigate their effects on catalysis or product specificity and diversity.[98] The genetic selection results showed that all of the mutations resulted in nonviable mutants, except for the *Sce*ERG7^{F699T} mutation, which suggested that Phe699 plays a crucial role in the catalysis. In addition, among the substitutions, only the *Sce*ERG7^{F699T} mutant produced novel protosta-13(17),24-dien-3β-ol as the sole truncated rearrangement product. Moreover, when Phe699 was substituted with a His residue, a new novel product, protosta-17(20),24-dien-3β-ol, in conjunction with lanosterol and protosta-13(17),24-dien-3β-ol, was isolated at a ratio of 17 : 13 : 70. The accumulation of tetracyclic protosta-13(17),24-dien-3β-ol and protosta-17(20),24-dien-3β-ol from the Phe699 mutants of *Sce*ERG7 clearly indicated the functional role of Phe699 in stabilizing the lanosteryl C-17 cation intermediate.[95,98] These two newly discovered tetracyclic structures also demonstrated the occurrence of putative truncated intermediate stages among the backbone rearrangement cascade, from protosteryl cation to the formation of lanosterol.

Recently, we applied a "contact mapping" strategy to identify amino acid residues within van der Waals radii for the C-8 carbon of the **OS** or lanosterol based on the assumption that amino acids within the active site surface are precedent to contribute to a catalytic outcome. Mutational studies of these residues may provide insight into the role of these residues in the determination of the B-ring configuration or in ring widening during C-ring formation. A particularly interesting Tyr residue was identified; it is located at the 707 position of *Sce*ERG7. In SHC, electrostatic stabilization created from the dipoles of the conserved Tyr609 and Tyr612 (which correspond to Tyr707 and Tyr710 of *Sce*ERG7, respectively), pointing to the early carbocation, has been proposed.[66] Substitutions of Tyr609 of *Aac*SHC with Ala resulted in accumulation of a truncated bicyclic cyclization intermediate, whereas the Phe substitution produced bicyclic, tetracyclic, and tetracyclic with one or two 1,2-hydride rearrangement products. Accumulation of bicyclic compound by the Tyr609 mutation suggested that Tyr609 is close to the position of the bicyclic C-8 cation in the enzyme cavity.[99] We then utilized site-saturated mutagenesis to investigate the effects, either steric or electrostatic, on the prefolded substrate conformation or the cation–π interactions. A novel C-B bicyclic intermediate, (9*R*,10*S*)-polypoda-8(26),13*E*,17*E*,21-tetraen-3β-ol, in addition to lanosterol, parkeol, and 9β-lanosta-7,24-dien-3β-ol, was isolated, for the first time, from the *Sce*ERG7^{Y707X} mutants (unpublished data). These results indicated that the Tyr707 residue might play an important role in stabilizing the C-B bicyclic C-8 cation and the final lanosteryl C-8/C-9 cation. Substitutions at this position interfered with the cyclization/rearrangement reaction cascade and resulted in the generation of a bicyclic triterpenoid and altered deprotonation products.

*Sce*ERG7 Homology Modeling and Correlation to the Oxidosqualene Cyclization/Rearrangement Mechanism

Due to the absence of a *Sce*ERG7 crystal structure, the elucidation of the relationship between the mutated enzyme and its product diversity is hampered. To provide some insight into the structural basis for the observed altered product specificity with the mutants, we generated structural homology models of wild-type and various *Sce*ERG7 mutants based on the crystal structures of *Aac*SHC and human OSC.[65,87] In addition, individual cationic intermediates or the respective annulated products were docked into the active site cavity of the wild-type and various mutated *Sce*ERG7 homology models. The superimposition of the *Sce*ERG7 homology modeling structure with the crystal structure of human OSC exhibited a similar secondary structure and three-dimensional profile, indicating that the overall skeleton was conserved among these mechanistic similar cyclases (Fig. 3A). A detailed investigation of the homology modeling structures suggested that a π-electron-rich pocket, which was created by previously illustrated catalytically important residues, including Tyr99, Trp232, His234, Trp390, Trp443, Phe445, Tyr510, Phe699, and Tyr707, coupled with other aromatic amino acid residues including Trp587, Tyr239, Trp194, Phe528, and Phe104, existed in the *Sce*ERG7 active site (Fig. 3B). Among these residues, His234 and Tyr510 were located on the top of the molecular plane of lanosterol and formed a hydrogen–bond dyad, from which Tyr510 was spatially near the C-8/C-9 position, whereas His234 was proximal to the C/D ring junction of lanosterol. Trp232 was positioned at the top half of the side wall of the active site cavity and proximal to the C-11, C-12, and C-13 orientations of lanosterol. Trp232 was also spatially close to His234 and Tyr510, and thought to affect the orientation of His234 as well as the His234:Tyr510 hydrogen–bond dyad. Phe445 was spatially proximal to both the B/C ring fusion and to the C-8 and C-14 positions, which are occupied directly above the cationic center during protosteryl cation formation. In addition, Trp443 was positioned spatially opposite Asp456, above the molecular plane of lanosterol, with a considerable distance (~10.1 Å) from the substrate. In contrast, Tyr99, Trp587, Phe699, and Tyr707 are located in the bottom half of the enzymatic active site cavity and in a position opposite that of the His234, Phe445, or Tyr510 residue.

According to the *Sce*ERG7 homology model, the hydroxyl group of Tyr510 was located at a distance of ~4.6 Å to the C-10 cation of the monocyclic intermediate (lanosterol numbering). This distance is in agreement with the dipoles for observed aromatic amino acid residues at a distance of 3.5 to 5.5 Å in the lanosterol-bound ERG7 complex (Fig. 4A). Thus, the mutagenic change on the position of Tyr510 might directly affect the cyclization cascade to produce achilleol A or the

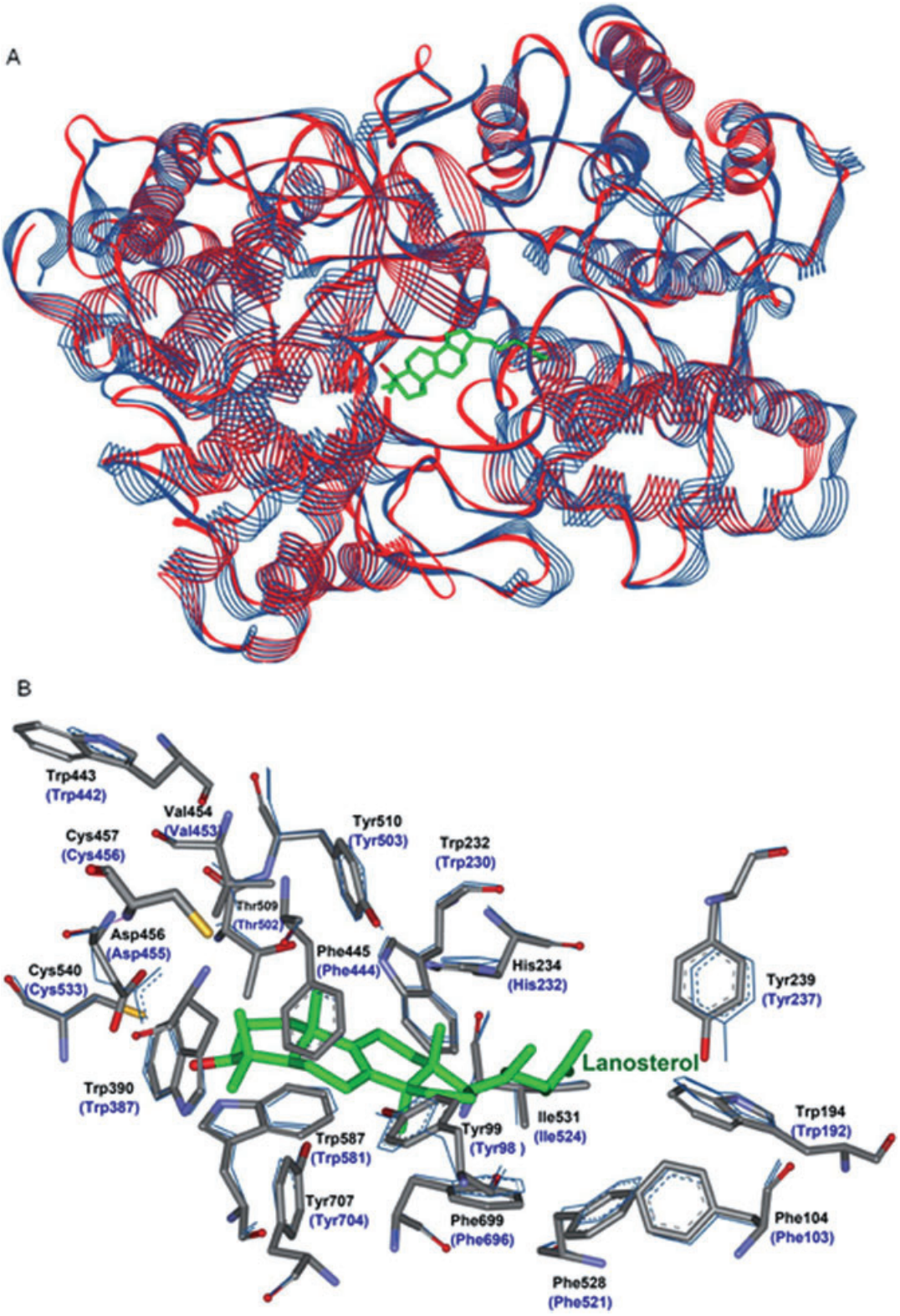

Fig. 3. (A) Superimposition of the *Saccharomyces cerevisiae* ERG7 (*Sce*ERG7) homology modeling structure (red) with the crystal structure of human oxidosqualene-lanosterol cyclase (OSC) (blue) and the docked product, lanosterol (green). (B) Local views of the superimposition of the homology model of *Sce*ERG7 (shown in stick representation and corresponding residues in black) with the human OSC crystal structure (shown in line representation in blue). For comparison, lanosterol (green) is also shown in the figure.

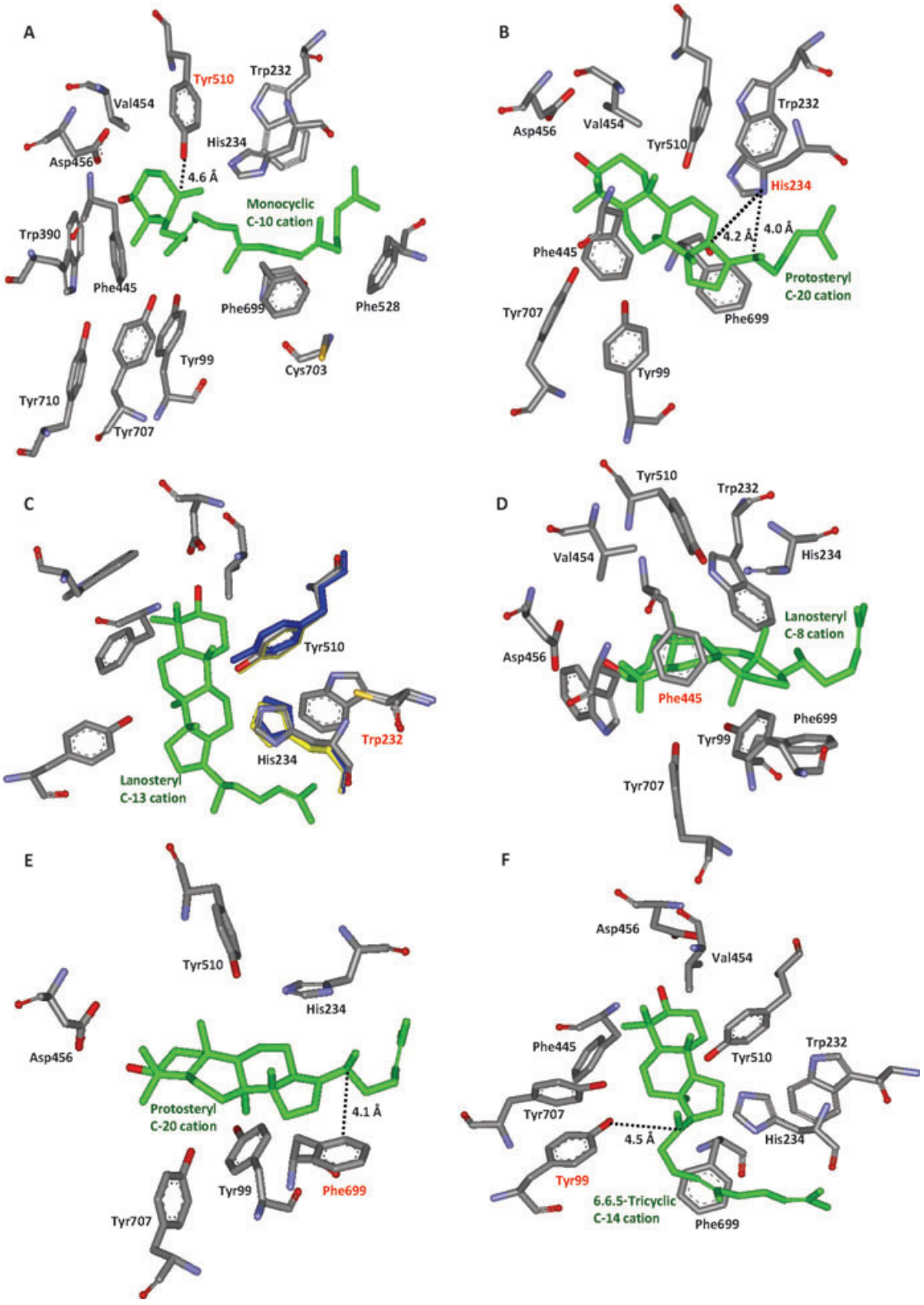

Fig. 4. (*Continued*)

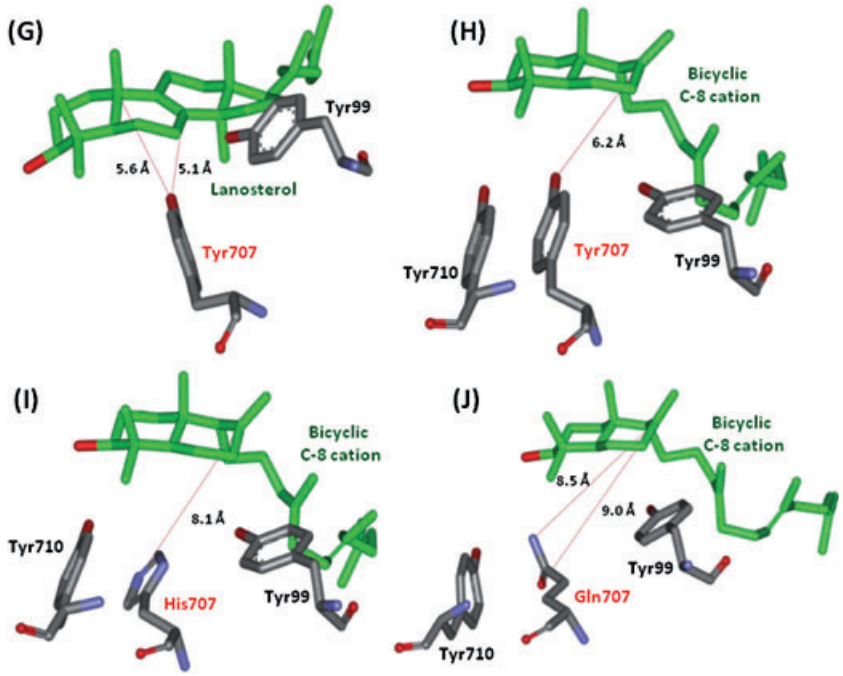

Fig. 4. Local view of the homology model of the *Saccharomyces cerevisiae* ERG7^{X} (*Sce*ERG7^{X}) structure. Putative active site residues (stick representation) are included. (A) The monocyclic C-10 cation is shown in green. The distance between the C-10 cation and phenolic oxygen of the Tyr510 residue is indicated by a dotted black line. (B) Lanosterol is shown in green, while the black dotted lines show the distance between the C-13 and C-20 positions of lanosterol with the Nε2 atom of His234, respectively. (C) Partially superimposed homology modeling structures of the wild-type *Sce*ERG7, *Sce*ERG7^{W232C}, and *Sce*ERG7^{W232A} proteins. The original His234:Tyr510 catalytic base dyad is shown with stick representation in gray, whereas yellow represents the Trp232Cys mutation and blue represents the Ala substitution. The lanosteryl C-13 cation is also shown. (D) Putative functional residues in the π-electron pocket of *Sce*ERG7 in which Phe445 is near the B/C ring junction. (E) Distance from the protosteryl C-20 cation to Phe699. (F) Distance from the tricyclic C-14 cation to Tyr99. (G) Distance from the lanosterol C-8 and lanosterol C-10 positions to the phenolic oxygen of Tyr707. (H) Distance from the bicyclic C-8 cation to the phenolic oxygen of Tyr707. (I) Distance from the bicyclic C-8 cation to the Nε2 atom of the His substitution. (J) Distance from the bicyclic C-8 cation to the amide group of the Gln substitution.

deprotonation to produce lanosterol and parkeol. The substitution of more bulky or basic amino acids on Tyr510 tended to produce monocyclic products, whereas the small or acidic amino acid substitutions favored polycyclic product formation. For example, the substitution of Tyr510 with His, Lys, Arg, and Trp caused steric or electronic repulsion to His234 and increased the production of monocyclic compounds. To our surprise, the *Sce*ERG7^{Y510W} mutant produced monocyclic but no polycyclic products.[100] Moreover, the isolation of (13α*H*)-isomalabarica-14(26),17*E*,21-trien-3β-ol implied the steric or electrostatic effect of the *Sce*ERG7^{Y510X} mutations on the His234 residue. Studies on the site-saturated mutagenesis of His234 showed that substitutions of the His234 position might influence the stabilization of the protosteryl C-20 and lanosteryl C-13 as well as the tricyclic Markovnikov tertiary C-14 cation, and thus result in the generation of a different ratio of achilleol A, (13α*H*)-isomalabarica-14(26),17*E*,21-trien-3β-ol, protosta-20,24-dien-3β-ol, protosta-12,24-dien-3β-ol, lanosterol, and parkeol. From the observation of the homology model, the position of the Nε2 of the His234 imidazole group was found at a distance of ~4.2 and 4.0 Å from the lanosteryl C-13 and protosteryl C-20 cations, respectively (Fig. 4B). Substitution of *Sce*ERG7^{H234} or *Sce*ERG7^{Y510} with other amino acid residues would predictably affect the steric or electrostatic interaction between the respective cationic intermediates and the active site residue side chains as well as the original His234:Tyr510 hydrogen-bonding network. When Tyr510 was changed into Asp, Asn, Glu, and Gln, an increased transient disturbance occurred between Tyr510 and His234, and subsequently influenced the orientation of His234 for stabilizing the C-14 cation.[94,95] This modified hydrogen-bonding network thus caused the steric or electrostatic influence to arrest the D-ring formation and also affected the stability of the tricyclic C-14 cationic intermediate, resulting in the generation of (13α*H*)-isomalabarica-14(26),17*E*,21-trien-3β-ol. Results from the ERG7$^{H234W/Y510V}$ and ERG7$^{H234W/Y510W}$ double mutants, from which the *Sce*ERG7$^{H234W/Y510W}$ double mutant produced almost 100% of

monocyclic product as that of the *Sce*ERG7^{Y510W} mutant, whereas abundant lanosterol production was observed in the *Sce*ERG7$^{H234W/Y510V}$ mutant, further supported the coordinative action of the hydrogen-bonding dyad. Moreover, the *Sce*ERG7^{H234W} mutant generated almost 100% of parkeol without any other cyclization products.[93] Interestingly, this kind of hydrogen-bonding pair in which either residue acts as the general base and influences the other for the deprotonation has been observed in the *Ath*CAS enzyme. The Tyr410 and His257 residues of *Ath*CAS were examined as the coordinative partners for the C-19 angular methyl proton abstraction.[91]

Alternatively, the catalytic importance of Trp232 might be implied via the indirect interactions from the spatially affected active site residues. Homology simulation of the Trp232 position with other residues showed that changes at this position reduce the π-electron density nearby and affect the interactions of active site residues, especially in the His234:Tyr510 catalytic base dyad hydrogen-bonding network, as well as shift the relative distance between the His234 and C-11/C-12 positions of lanosterol. Obviously, the distance from His234 to the lanosteryl C-13 cation was changed and was closer to the C-11 and C-12 position of the lanosteryl cation. Thus, the alternatively deprotonated products, either parkeol or protosta-12,24-dien-3β-ol, were respectively generated in the replacement of the bulky Trp232 to the smaller residues (Fig. 4C).[97]

The tricyclic (13α*H*)-isomalabarica-14(26),17*E*,21-trien-3β-ol and three altered deprotonation products, lanosterol, parkeol, and 9β-lanosta-7,24–3β-ol, were also observed from the product profiles in the *Sce*ERG7^{F445X} mutants (*X* = Cys, Met, Asp, Asn, and Thr).[101] Careful examination of the mutants' homology models suggested that the electronic differences between Phe445 and the polar side-chain groups of similarly sized amino acid residues could account for the catalytic differences in the formation of various products (Fig. 4D). In addition to the spatial proximity of Phe445 to the B/C ring junction and proximity to the C-8/C-14 positions, Phe445 also exhibited a definitive interaction with other individual π-electron-rich aromatic residues, including Tyr99 (3.7 Å), Trp390 (4.4 Å), Tyr510 (6.5 Å), Tyr707 (4.0 Å), and Tyr710 (6.2 Å), within the cyclase active site. Because these aromatic residues were proposed as providing the high electron density gradient for the equilibrium shift toward the final deprotonation reaction at the lanosteryl C-8/C-9 cation, substitution of Phe445 might partially disturb the transient cation–π interaction during the rearrangement step, affect the equilibrium tendency for the C-8/C-9 proton position, and consequently result in the formation of three possibly altered deprotonation products.[87,90] Alternatively, although the relative distances from Phe445 or His234 to the lanosteryl C-8 cation were both approximately 5 Å, the difference of product profiles between the Phe445 and His234 substituted mutants could be rationalized from an elucidation of the homology models. His234 exhibited the obvious hydrogen-bonding interaction for the Tyr510 residue, whereas the hydrogen bond was absent between the Phe445 and Tyr510 residues due to the long distance of approximately 6.5 Å.[101] The effects caused by the Phe445 substitution on either the steric orientation of the Tyr510 position or on the intrinsic Tyr510:His234 hydrogen-bonding interactions were not observed in the *Sce*ERG7^{F445X} mutants. The spatially altered active site cavity structure and the affected electrostatic interaction between the His234:Tyr510 hydrogen-bonding network was only observed in the His234 substitutions.[92,93]

In our laboratory, several newly truncated cyclization bicyclic and tricyclic as well as the truncated rearrangement tetracyclic products, including bicyclic (9*R*,10*S*)-polypoda-8(26),13*E*,17*E*,21-tetraen-3β-ol, tricyclic (13α*H*)-isomalabarica-14*Z*,17*E*,21-trien-3β-ol, (13α*H*)-isomalabarica-14*E*,17*E*,21-trien-3β-ol, protosta-13(17),24-dien-3β-ol, and tetracyclic protosta-17(20),24-dien-3β-ol, were respectively isolated from either Tyr99, Phe699, or Tyr707 mutants.[93,96,102] Although the exact reasons for the production of diverse products in different *Sce*ERG7 mutants are complicated, the illustration of the structural basis obtained through the homology modeling might provide suitable insight for examining the experimental results. As previously described, the Tyr99, Phe699, and Tyr707 residues were all located in the bottom half of the enzymatic active site cavity and in the opposite position relative to the His234, Phe445, and Tyr510 residues. In addition, Tyr99 occupied the middle site in the cavity and interacted with the substrate via its phenolic oxygen side chain. The distance between the phenolic oxygen of Tyr99 and the tricyclic Markovnikov C-14 cation was approximately 4.5 Å, while Phe699 showed a very similar distance (4.1 Å) to the tetracyclic lanosteryl C-17 cation (Fig. 4E,F). The short distance allows these two amino acids to stabilize the electron-deficient C-14 or C-17 cationic intermediates during the annulations of the C/D ring, respectively. Thus, the simultaneous isolation of different stereochemically (13α*H*)-isomalabarica-14*Z*,17*E*,21-trien-3β-ol and (13α*H*)-isomalabarica-14*E*, 17*E*,21-trien-3β-ol from the *Sce*ERG7^{Y99X} mutants indicated that the affected enzymatic active site allows a slight rotation of the long carbon side chain along the axis of the C-14/C-15 backbone, resulting in the incorrect deprotonation process. Interestingly, the totally different product profiles between the experimental results of the *Sce*ERG7^{Y99} mutants and the theoretical speculation for the corresponding Tyr98 from human OSC crystal structure might indicate an imperceptible discrepancy or a different spatial neighboring assistance in these two eukaryotic lanosterol cyclases. However, other factors assisting the substrate folding, including the steric or electrostatic effect, could not be excluded.

In other experiments, a long-awaited bicyclic intermediate structure, (9*R*,10*S*)-polypoda-8(26),13*E*,17*E*,21-tetraen-3β-

ol, which was generated after the ERG7-mediated concerted epoxide ring opening/A-ring cyclization coupled with the arrest at the bicyclic step, was isolated from our recent site-saturated mutants on the Tyr707 residue.[102] The newly trapped bicyclic product, together with three altered deprotonation products including lanosterol, parkeol, and 9β-lanosta-7,24-dien-3β-ol, was identified from various *Sce*ERG7^{Y707X} mutants. The results indicated that the Tyr707 residue might play an important role in stabilizing the C-8 cation during the formation of the second cyclohexyl ring and the final lanosteryl C-8/C-9 cation. Substitutions at this position interrupted the cyclization cascade to generate the bicyclic triterpenoid alcohol and interfered with the deprotonation step to generate the other three altered deprotonation products. The homology model of the *Sce*ERG7 model showed a relative distance of 5.1 and 6.2 Å between the hydroxyl group of Tyr707 and the lanosterol C-8 position and bicyclic C-8 cation, respectively (Fig. 4G,H). In addition, the distance between the bicyclic C-8 cation and the phenolic oxygen of Tyr was increased to about 8.1 and 9.0 Å when Tyr707 was substituted with His and Gln, respectively (Fig. 4I,J). The greater distance apparently caused the loss of the cation–π interaction and destabilized the carbocation, resulting in facilitated deprotonation and accumulation of bicyclic truncated product. The crucial importance of Tyr707 in the formation of the truncated bicyclic C-B triterpene alcohol and the contradictive role between Tyr707 of yeast ERG7 and Tyr98 of human OSC should be further clarified. However, from the observation of yeast ERG7 homology structure or human OSC structure, the positions of Tyr707 and/or Tyr99 are the only functional residues that occupied an orientation suitable for enforcing the conformation of the secondary cyclohexyl ring into a boat form.

Conclusion

In summary, the parallel identification of relevant residues critical in both OSC and CAS catalysis revealed their importance in oxidosqualene cyclization/rearrangement reactions. In addition, the functional role of these residues in the ERG7-templated oxidosqualene cyclization/rearrangement cascade is summarized as follows: (i) Asp456 coupled with two cysteine residues (Cys457 and Cys540) were crucial for the initiation step in the ERG7-catalyzed reaction; (ii) Trp443, spatially opposite Asp4556, might play a role in influencing substrate binding, stabilizing epoxide protonation, and inducing A-ring formation; (iii) Val454 also contributed the steric effect of assisting in the orientation of substrate during cyclization;[103] (iv) after the oxirane ring opening and A-ring cyclization, Tyr510 provided functional importance in stabilizing the monocyclic C-10 cationic intermediate; (v) the subsequent cation-π annulation generated the C-B bicyclic C-8 cation and the C-B 6,6,5-Markovnikov tricyclic C-14 cation, which were stabilized by Tyr707, Tyr99, and His234 residues, respectively; (vi) His234 and Phe699 further provided highly electronic propriety to stabilize the D-ring closured protosteryl C-20 cation as well as the first hydride rearranged lanosteryl C-17 cation; (vii) Trp232, the neighboring residue of His234, showed its unequivocal importance in the rearrangement process and also exhibited an influence on the coordinative action between His234 and Tyr510; (viii) in addition to stabilization of the respective carbocationic intermediates during the different stages of the cyclization process, His234 and Tyr510 further displayed a crucial role in guiding the final deprotonation; and (ix) Phe445 influenced both the C-ring formation and deprotonation step. This is distinct from the function of His234 that was suggested according to the structural insight. In addition, data from these experiments demonstrate how minor changes in an enzyme active site can alter product specificity and further highlight the potential for increasing the diversity of triterpene skeletons through molecular evolution and metabolic engineering of the cyclase enzyme family. Finally, the subtle size or electrostatic changes of the active site environment that influenced the structure–function relationships of the cyclase enzymes could only be thoroughly analyzed by the utilization of site-saturated mutagenesis coupled with product isolation and characterization.

Future Perspectives

Oxidosqualene Cyclase-Catalyzed Cyclization/ Rearrangement Mechanism

Data obtained from bioorganic, biochemical, biophysical, and molecular genetic approaches have greatly advanced our understanding of the OSC-catalyzed reaction, particularly regarding the functional residues responsible for required critical steps and truncated cyclization/rearrangement structures hypothetically postulated within the overall cyclization cascade. However, many areas of interest remain unsolved including (i) how enzymes sterically control C-B-C vs. C-C-C substrate prefolded conformations for different pathways of cyclization; (ii) the concerted or nonconcerted A/B ring cyclization; (iii) the asynchronous concerted bicyclic vs. tricyclic cyclopentylcarbinylcyclohexyl to tetracyclic protosteryl cation cyclization mechanism; (iv) the stereochemical course of the C-17α/β orientation and C-20*R/S* configuration of the protosteryl cation; (v) the functional residues involved in stabilizing the lanosteryl C-14 cation; and (vi) the critical residues in determining product specificity toward cyclopropyl ring closure or different deprotonations. Moreover, approaches utilizing directed evolution coupled with the *erg7*-deficient yeast strain also provide an opportunity to select β-amyrin synthase or lupeol synthase

genes possessing lanosterol- or novel product-synthetic ability, and/or to identify critical residues involved in defining the course of the complex cyclization/rearrangement cascade.

Structural Biology

The first crystal structure of human OSC has provided valuable structural insights for illustrating the molecular interactions between lanosterol and enzymatic active sites. Bioinformatic tools have also assisted in creating plausible homology models based on this crystal structure to elucidate the importance of critical amino acids in *Sce*ERG7-catalyzed cyclization. However, recent site-saturated mutagenesis and the analysis of diverse products generated from various *Sce*ERG7 mutants revealed a contradictory situation between human OSC crystal structure and *Sce*ERG7 homology models. The data suggested that a slightly altered orientation might exist between the active site cavity of human OSC and *Sce*ERG7. In addition, there were repeat observations of multiple products arising from the different *Sce*ERG7 mutants. Further, the mutated cyclase produced the altered products with the deprotonation position, which is unexpectedly distinct from that of the mutated site, indicating the influence of other amino acids in these single point mutations.

The structural determination of fungal oxidosqualene cyclases is a major priority in the development of antifungal drugs. In order to understand the role of functional residues assisting in substrate binding, cationic intermediate stabilization, and coordinative interaction with other amino acids in an in-depth way, as well as for the rational design of antifungal drugs, determination of the three-dimensional structures of these mutated cyclases is necessary. The *Pichia pastoris* expression system has been used for elucidating the crystal structure of human OSC. This expression system might be a suitable candidate system for the expression and crystallization of different *Sce*ERG7 mutants. Moreover, the isolated partially cyclized products might be used for the co-crystallization and detailed understanding of the molecular interactions between enzymatic active sites and the various products.

Molecular Evolution of Oxidosqualene Cyclases for Protein Plasticity and Product Diversity

Mutagenesis studies demonstrated that the variation of cyclization reactions could be attained by only a small modification of enzymatic active sites. In addition, sequence comparison and the homology models suggested that some specific domains in the enzymatic active sites might be responsible for product specificity. Interestingly, various mutated cyclases (e.g., *Sce*ERG7^{H234S} and *Sce*ERG7^{H234T}) have been examined for their altered product specificity from original lanosterol synthase into either protosta-12,24-dien-3β-ol synthase or parkeol synthase, whereas *Ath*CAS$^{H477N/I481V}$ exhibited a nearly 100% product conversion from cycloartenol into lanosterol.[86,93] Moreover, functional genomic studies on the putative OSC homologous gene from the *A. thaliana* genome have characterized many cyclase proteins with novel catalytic functions.[81,104–114] Recent papers have introduced the detailed reaction mechanism and molecular origin of structural diversity concerning the newly discovered oxidosqualene cyclases in plants.[107,113,115] Careful elucidation of the sequence alignment of these cyclases and comparison with other function-known cyclases might provide valuable information for the catalytic distinctions among cyclase-catalyzed reactions. Thus, different artificial cyclases with new catalytic activity or novel product specificity/diversity could theoretically be generated via diverse genetic selection or molecular evolution methods. Moreover, rationally designed cyclase enzymes could also be obtained by structure-based alteration after a well-designed analysis of product specificity-determining catalytic residues, which will be revealed in the future from an array of three-dimensional protein structures.

REFERENCES

[1] Connolly, J. D.; Hill, R. A. Nat Prod Rep 2002, 19, 494.
[2] Xu, R.; Fazio, G. C.; Matsuda, S. P. T. Phytochemistry 2004, 65, 261.
[3] Abe, I.; Rohmer, M.; Prestwich, G. D. Chem Rev 1993, 93, 2189.
[4] Wendt, K. U.; Schulz, G. E.; Corey, E. J.; Liu, D. R. Angew Chem Int Ed 2000, 39, 2812.
[5] Eschenmoser, A.; Ruzicka, L.; Jeger, O.; Arigoni, D. Helv Chim Acta 1955, 38, 1890.
[6] Stork, G.; Burgstahler, A. W. J Am Chem Soc 1955, 77, 5068.
[7] Segura, M. J.; Jackson, B. E.; Matsuda, S. P. T. Nat Prod Rep 2003, 20, 304.
[8] Woodward, R. B.; Bloch, K. J Am Chem Soc 1953, 75, 2023.
[9] Maudgal, R. K.; Tchen, T. T.; Bloch, K. J Am Chem Soc 1958, 80, 2589.
[10] Cornforth, J. W.; Cornforth, R. H.; Donninger, C.; Popjak, G.; Shimizu, Y.; Ichii, S.; Forchielli, E.; Caspi, E. J Am Chem Soc 1965, 87, 3224.
[11] Corey, E. J.; Russey, W. E.; Ortiz de Montellano, P. R. J Am Chem Soc 1966, 88, 4750.
[12] van Tamelen, E. E.; Willett, J. D.; Clayton, R. B.; Lord, K. E. J Am Chem Soc 1966, 88, 4752.
[13] Willett, J. D.; Sharpless, K. B.; Lord, K. E.; van Tamelen, E. E.; Clayton, R. B. J Biol Chem 1967, 242, 4182.
[14] van Tamelen, E. E.; Willet, J.; Schwartz, M.; Nadeau, R. J Am Chem Soc 1966, 88, 5937.

[15] Barton, D. H. R.; Jarman, T. R.; Watson, K. C.; Widdowson, D. A.; Boar, R. B.; Damps, K. J Chem Soc, Perkin Trans 1 1975, 1134.
[16] Corey, E. J.; Russey, W. E. J Am Chem Soc 1966, 88, 4751.
[17] Corey, E. J.; Ortiz de Montellano, P. R.; Lin, K.; Dean, P. D. G. J Am Chem Soc 1967, 89, 2797.
[18] Corey, E. J.; Gross, S. K. J Am Chem Soc 1967, 89, 4561.
[19] Clayton, R. B.; van Tamelen, E. E.; Nadeau, R. G. J Am Chem Soc 1968, 90, 820.
[20] Corey, E. J.; Lin, K.; Jautelat, M. J Am Chem Soc 1968, 90, 2724.
[21] Anding, C.; Heintz, R.; Ourisson, G. C R Acad Sci Hebd Seances Acad Sci D 1973, 276, 205.
[22] Bujons, J.; Guajardo, R.; Kyler, K. S. J Am Chem Soc 1988, 110, 604.
[23] Xiao, X. Y.; Prestwich, G. D. Tetrahedron Lett 1991, 32, 6843.
[24] Boutaud, O.; Dolis, D.; Schuber, F. Biochem Biophys Res Commun 1992, 188, 898.
[25] Corey, E. J.; Virgil, S. C.; Liu, D. R.; Sarshar, S. J Am Chem Soc 1992, 114, 1524.
[26] Ceruti, M.; Balliano, G.; Viola, F.; Grosa, G.; Rocco, F.; Cattel, L. J Med Chem 1992, 35, 3050.
[27] Balliano, G.; Milla, P.; Ceruti, M.; Viola, F.; Carrano, L.; Cattel, L. FEBS Lett 1993, 320, 203.
[28] van Tamelen, E. E.; James, D. R. J Am Chem Soc 1977, 99, 950.
[29] van Tamelen, E. E.; Hopla, R. E. J Am Chem Soc 1979, 101, 6112.
[30] Ceruti, M.; Rocco, F.; Viola, F.; Balliano, G.; Milla, P.; Arpicco, S.; Cattel, L. J Med Chem 1998, 41, 540.
[31] Corey, E. J.; Cheng, H.; Baker, C. H.; Matsuda, S. P. T.; Li, D.; Song, X. J Am Chem Soc 1997, 119, 1277.
[32] Corey, E. J.; Virgil, S. C.; Cheng, H.; Baker, C. H.; Matsuda, S. P. T.; Singh, V.; Sarshar, S. J Am Chem Soc 1995, 117, 11819.
[33] van Tamelen, E. E.; Sharpless, K. B.; Hanzlik, R. P.; Clayton, R. B.; Burlingame, A. L.; Wszolek, P. C. J Am Chem Soc 1967, 89, 7150.
[34] Corey, E. J.; Cheng, H. Tetrahedron Lett 1996, 37, 2709.
[35] Hoshino, T.; Sakai, Y. Chem Commun 1998, 1591.
[36] Hoshino, T.; Kouda, M.; Abe, T.; Ohashi, S. Biosci Biotechnol Biochem 1999, 63, 2038.
[37] Matsuda, S. P. T.; Wilson, W. K.; Xiong, Q. Org Biomol Chem 2006, 4, 530.
[38] Corey, E. J.; Virgil, S. C. J Am Chem Soc 1991, 113, 4025.
[39] Corey, E. J.; Virgil, S. C.; Sarshar, S. J Am Chem Soc 1991, 113, 8171.
[40] van Tamelen, E. E.; Murphy, J. W. J Am Chem Soc 1970, 92, 7204.
[41] Nes, W. R. Lipid 1974, 9, 596.
[42] Rohmer, M.; Bouvier, P.; Ourisson, G. Proc Natl Acad Sci USA 1979, 76, 847.
[43] Ourisson, G.; Rohmer, M.; Poralla, K. Ann Rev Microbiol 1987, 41, 301.
[44] Ourisson, G. Pure & Appl Chem 1989, 61, 345.
[45] Johnson, W. S. Tetrahedron 1991, 47, xi.
[46] Johnson, W. S.; Telfer, S. J.; Cheng, S.; Schubert, U. J Am Chem Soc 1987, 109, 2517.
[47] Ochs, D.; Kaletta, C.; Entian, K.-D.; Beck-Sickinger, A.; Poralla, K. J Bacteriol 1992, 174, 298.
[48] Buntel, C. J.; Griffin, J. H. J Am Chem Soc 1992, 114, 9711.
[49] Roessner, C. A.; Min, C.; Hardin, S. H.; Harris-Haller, L. W.; McCollum, J. C.; Scott, A. I. Gene 1993, 127, 149.
[50] Corey, E. J.; Matsuda, S. P. T.; Bartel, B. Proc Natl Acad Sci USA 1994, 91, 2211.
[51] Shi, Z.; Buntel, C. J.; Griffin, J. H. Proc Natl Acad Sci USA 1994, 91, 7370.
[52] Corey, E. J.; Matsuda, S. P. T.; Baker, C. H.; Ting, A. Y.; Cheng, H. Biochem Biophys Res Commun 1996, 219, 327.
[53] Abe, I.; Bai, M.; Xiao, X. Y.; Prestwich, G. D. Biochem Biophys Res Comm 1992, 187, 32.
[54] Baker, C. H.; Matsuda, S. P. T.; Liu, D. R.; Corey, E. J. Biochem Biophys Res Commun 1995, 213, 154.
[55] Kusano, M.; Shibuya, M.; Sankawa, U.; Ebizuka, Y. Biol Pharm Bull 1995, 18, 195.
[56] Corey, E. J.; Matsuda, S. P.; Bartel, B. Proc Natl Acad Sci USA 1993, 90, 11628.
[57] Kushiro, T.; Shibuya, M.; Ebizuka, Y. Eur J Biochem 1998, 256, 238.
[58] Poralla, K. Bioorg & Medicinal Chem Lett 1994, 4, 285.
[59] Poralla, K.; Hewelt, A.; Prestwich, G. D.; Abe, I.; Reipen, I.; Sprenger, G. Trends Biochem Sci 1994, 19, 157.
[60] Dougherty, D. A.; Stauffer, D. A. Science 1990, 250, 1558.
[61] McCurdy, A.; Jimenez, L.; Stauffer, D. A.; Dougherty, D. A. J Am Chem Soc 1992, 114, 10314.
[62] Kumpf, R. A.; Dougherty, D. A. Science 1993, 261, 1708.
[63] Dougherty, D. A. Science 1996, 271, 163.
[64] Wendt, K.-U.; Feil, C.; Lenhart, A.; Poralla, K.; Schulz, G. E. Protein Sci 1997, 6, 722.
[65] Wendt, K. U.; Poralla, K.; Schulz, G. E. Science 1997, 277, 1811.
[66] Wendt, K. U.; Lenhart, A.; Schulz, G. E. J Mol Biol 1999, 286, 175.
[67] Reinert, D. J.; Balliano, G.; Schulz, G. E. Chem Biol 2004, 11, 121.
[68] Feil, C.; Süssmuth, R.; Jung, G.; Poralla, K. Eur J Biochem 1996, 242, 51.
[69] Sato, T.; Abe, T.; Hoshino, T. Chem Comm 1998, 2617.
[70] Pale-Grosdemange, C.; Feil, C.; Rohmer, M.; Poralla, K. Angew Chem Int Ed 1998, 37, 2237.
[71] Sato, T.; Hoshino, T. Biosci Biotechnol Biochem 1999, 63, 2189.
[72] Merkofer, T.; Pale-Grosdemange, C.; Rohmer, M.; Poralla, K. Tetrahedron Lett 1999, 40, 2121.
[73] Pale-Grosdemange, C.; Merkofer, T.; Rohmer, M.; Poralla, K. Tetrahedron Lett 1999, 40, 6009.
[74] Lenhart, A.; Weihofen, W. A.; Pleschke, A. E.; Schulz, G. E. Chem Biol 2002, 9, 639.
[75] Hoshino, T.; Sato, T. Chem Comm 2002, 291.
[76] Abe, I.; Prestwich, G. D. J Biol Chem 1994, 269, 802.

[77] Corey, E. J.; Cheng, H.; Baker, C. H.; Matsuda, S. P. T.; Li, D.; Song, X. J Am Chem Soc 1997, 119, 1289.
[78] Xiao, X.; Prestwich, G. D. J Am Chem Soc 1991, 113, 9673.
[79] Abe, I.; Dang, T.; Zheng, Y. F.; Madden, B. A.; Fei, C.; Poralla, K.; Prestwich, G. D. J Am Chem Soc 1997, 119, 11333.
[80] Hart, E. A.; Hua, L.; Darr, L. B.; Wilson, W. K.; Pang, J.; Matsuda, S. P. T. J Am Chem Soc 1999, 121, 9887.
[81] Matsuda, S. P. T.; Darr, L. B.; Hart, E. A.; Herrera, J. B. R.; McCann, K. E.; Meyer, M. M.; Pang, J.; Schepmann, H. G.; Wilson, W. K. Org Lett 2000, 2, 2261.
[82] Herrera, J. B. R.; Wilson, W. K.; Matsuda, S. P. T. J Am Chem Soc 2000, 122, 6765.
[83] Wu, T. K.; Griffin, J. H. Biochemistry 2002, 41, 8238.
[84] Meyer, M. M.; Xu, R.; Matsuda, S. P. T. Org Lett 2002, 4, 1395.
[85] Segura, M. J. R.; Lodeiro, S.; Meyer, M. M.; Patel, A. J.; Matsuda, S. P. T. Org Lett 2002, 4, 4459.
[86] Lodeiro, S.; Schulz-Gasch, T.; Matsuda, S. P. T. J Am Chem Soc 2005, 127, 14132.
[87] Thoma, R.; Schulz-Gasch, T.; D'Arcy, B.; Benz, J.; Aebi, J.; Dehmlow, H.; Hennig, M.; Stihle, M.; Ruf, A. Nature 2004, 432, 118.
[88] Corey, E. J.; Virgil, S. C. J Am Chem Soc 1990, 112, 6429.
[89] Wendt, K. U. Angew Chem Int Ed 2005, 44, 3966.
[90] Schulz-Gasch, T.; Stahl, M. J Comput Chem 2003, 24, 741.
[91] Lodeiro, S.; Segura, M. J.; Stahl, M.; Schulz-Gasch, T.; Matsuda, S. P. T. ChemBioChem 2004, 5, 1581.
[92] Wu, T. K.; Liu, Y. T.; Chang, C. H. ChemBioChem 2005, 6, 1177.
[93] Wu, T. K.; Liu, Y. T.; Chang, C. H.; Yu, M. T.; Wang, H. J. J Am Chem Soc 2006, 128, 6414.
[94] Lodeiro, S.; Wilson, W. K.; Shan, H.; Matsuda, S. P. T. Org Lett 2006, 8, 439.
[95] Wen, H. Y. Studies of Structure-Reactivity Relationships on Putative Active Site Cavity Residues of Oxidosqualene-Lanosterol Cyclase by Site-saturated Mutagenesis; Department of Biological Science and Technology, National Chiao Tung University: Hsin-Chu, Taiwan, 2007.
[96] Li, W. H. Site-saturated Mutagenesis Approach to Investigate the Putative Active-Site Residues from Saccharomyces cerevisiae Oxidosqualene-Lanosterol Cyclase that Influences the Cyclization/Rearrangement Reactions; Department of Biological Science and Technology, National Chiao Tung University: Hsin-Chu, Taiwan, 2007.
[97] Wu, T. K.; Yu, M. T.; Liu, Y. T.; Chang, C. H.; Wang, H. J.; Diau, E. W. G. Org Lett 2006, 8, 1319.
[98] Wu, T. K.; Wen, H. Y.; Chang, C. H.; Liu, Y. T. Org Lett 2008, 10, 2529.
[99] Sato, T.; Hoshino, T. Biosci Biotechnol Biochem 2001, 65, 2233.
[100] Wu, T. K.; Chang, C. H. ChemBioChem 2004, 5, 1712.
[101] Wu, T. K.; Liu, Y. T.; Chiu, F. H.; Chang, C. H. Org Lett 2006, 8, 4691.
[102] Wang, T. T. Tyrosine 707 within Ooxidosqualene-Lanosterol Cyclase from Saccharomyces cerevisiae Influences B-ring Formation and Deprotonation Reactions, Department of Biological Science and Technology, National Chiao Tung University: Hsin-Chu, Taiwan, 2008.
[103] Joubert, B. M.; Hua, L.; Matsuda, S. P. T. Org Lett 2000, 2, 339.
[104] Segura, M. J.; Meyer, M. M.; Matsuda, S. P. Org Lett 2000, 2, 2257.
[105] Kushiro, T.; Shibuya, M.; Masuda, K.; Ebizuka, Y. J Am Chem Soc 2000, 122, 6816.
[106] Xiong, Q.; Wilson, W. K.; Matsuda, S. P. Angew Chem Int Ed Engl 2006, 45, 1285.
[107] Phillips, D. R.; Rasbery, J. M.; Bartel, B.; Matsuda, S. P. Curr Opin Plant Biol 2006, 9, 305.
[108] Kolesnikova, M. D.; Xiong, Q.; Lodeiro, S.; Hua, L.; Matsuda, S. P. Arch Biochem Biophys 2006, 447, 87.
[109] Xiang, T.; Shibuya, M.; Katsube, Y.; Tsutsumi, T.; Otsuka, M.; Zhang, H.; Masuda, K.; Ebizuka, Y. Org Lett 2006, 8, 2835.
[110] Kolesnikova, M. D.; Obermeyer, A. C.; Wilson, W. K.; Lynch, D. A.; Xiong, Q.; Matsuda, S. P. Org Lett 2007, 9, 2183.
[111] Kolesnikova, M. D.; Wilson, W. K.; Lynch, D. A.; Obermeyer, A. C.; Matsuda, S. P. Org Lett 2007, 9, 5223.
[112] Lodeiro, S.; Xiong, Q.; Wilson, W. K.; Kolesnikova, M. D.; Onak, C. S.; Matsuda, S. P. J Am Chem Soc 2007, 129, 11213.
[113] Shibuya, M.; Xiang, T.; Katsube, Y.; Otsuka, M.; Zhang, H.; Ebizuka, Y. J Am Chem Soc 2007, 129, 1450.
[114] Shan, H.; Wilson, W. K.; Phillips, D. R.; Bartel, B.; Matsuda, S. P. Org Lett 2008, 10, 1897.
[115] Abe, I. Nat Prod Rep 2007, 24, 1311.